

석 사 학 위 논 문

Master Thesis

박막의 굽힘 거동 측정을 위한

순수 굽힘 장비 개발

Development of a pure bending equipment for measuring
the bending behavior of thin films

2023

배 준 한 (裴 俊 漢 Bae, Junhan)

한 국 과 학 기 술 원

Korea Advanced Institute of Science and Technology

석 사 학 위 논 문

박막의 굽힘 거동 측정을 위한
순수 굽힘 장비 개발

2023

배 준 한

한 국 과 학 기 술 원

기계항공공학부/기계공학과

박막의 굽힘 거동 측정을 위한
순수 굽힘 장비 개발

배 준 한

위 논문은 한국과학기술원 석사학위논문으로
학위논문 심사위원회의 심사를 통과하였음

2022년 12월 20일

심사위원장 이 필 승 (인)

심 사 위 원 윤 정 환 (인)

심 사 위 원 김 효 진 (인)

Development of a pure bending equipment for measuring the bending behavior of thin films

Bae, Junhan

Advisor: Phill-Seung Lee

A thesis submitted to the faculty of
Korea Advanced Institute of Science and Technology in
partial fulfillment of the requirements for the degree of
Master of Science in Mechanical Engineering

Daejeon, Korea
December 20, 2022

Approved by

Phill-Seung Lee
Professor of Mechanical Engineering

The study was conducted in accordance with Code of Research Ethics¹⁾.

1) Declaration of Ethical Conduct in Research: I, as a graduate student of Korea Advanced Institute of Science and Technology, hereby declare that I have not committed any act that may damage the credibility of my research. This includes, but is not limited to, falsification, thesis written by someone else, distortion of research findings, and plagiarism. I confirm that my dissertation contains honest conclusions based on my own careful research under the guidance of my advisor.

MME

배준한. 박막의 굽힘 거동 측정을 위한 순수 굽힘 장비 개발.
기계항공공학부/기계공학과. 2023년. 42+iii 쪽. 지도교수: 이필승.
(영문 논문)

Bae, Junhan. Development of a pure bending equipment for measuring the bending behavior of thin films. Department of Mechanical Engineering. 2023. 42+iii pages. Advisor: Lee, Phill-Seung. (Text in English)

Abstract

With the development of thin film manufacturing technology, it is changing from rigid substrate products to flexible products that can transform the shape of products. Examples of products using this flexible thin film can be used in various fields such as organic photocells, substrate printing, and display technology, and play an important role in the development and research of materials with new properties. However, thin films used in industry are rarely designed to withstand external stress and are vulnerable to external stress due to their thin structure. In order to solve the problem of mechanical reliability of products using thin films, it is essential to understand the mechanical properties of thin films to predict and prevent mechanical damage to products. Thin film structures do not exist alone in the actual environment, but in the actual process of laminating other materials, such as substrates, residual stress occurs due to the interaction between the thin film and the substrate, resulting in bending behavior. In addition, since the main behavior of flexible devices manufactured using a thin film is the bending behavior, it is necessary to measure the bending behavior of the thin film. In this thesis, we propose a pure bending device for measuring the bending behavior of a thin film. The moment-curvature diagram generated by the bending of the thin film was shown through the developed experimental equipment, and the flexural rigidity, which is a mechanical property related to the bending behavior of the thin film, was measured through the diagram. In addition, two experimental verifications were conducted to secure the reliability of the designed experimental equipment, and as a result, the reliability of the designed experimental equipment was secured.

Keywords: Thin film, Pure bending, Bending behavior, Moment-curvature diagram, Flexural rigidity

Contents

Contents	i
List of Tables	ii
List of Figures	iii
Chapter 1. Introduction	1
Chapter 2. Equipment design	3
2.1 Requirements for pure bending	3
2.2 Equipment design process	4
Chapter 3. Experimental verification	17
3.1 Pure bending test	17
3.2 Tensile test	22
3.3 Young's modulus comparison	28
3.4 Moment-curvature diagram comparison	30
3.5 Material nonlinearity	34
Chapter 4. Conclusions	36
Bibliography	38
Acknowledgments in Korean	42

List of Tables

Table 2.1 Torque Meter Specification	16
Table 3.1 Materials for the experiment	19
Table 3.2 Results for each material (Unit: kgf·cm)	19
Table 3.3 Results for each material (Unit: N·mm)	20
Table 3.4: Mechanical properties for the experiment	27
Table 3.5 Regression results for each material	29
Table 3.6 Results of Young's modulus comparison	29
Table 3.7 Regression results for each material (Four layers)	35

List of Figures

Fig. 2.1 Requirements for pure bending	3
Fig. 2.2 Jigs for fixing the vertical state of the specimen	4
Fig. 2.2 Pure bending of specimen	5
Fig. 2.3 Deformed shapes of specimen	5
Fig. 2.4 Deformed shapes of specimen in XY Plane	6
Fig. 2.5 Definition of displacement and theta of thin film when the specimen is bent	7
Fig. 2.6 Deformed shapes and trace of of the free end of the thin film when the thin film is bent	7
Fig. 2.7 3D modeling design of the 1st version prototype (a) Isometric view, (b) Top view	8
Fig. 2.8 1st version equipment	9
Fig. 2.9 Arc and jig holes (Top view)	10
Fig. 2.10 Arc and jig holes (Enlarge view)	10
Fig. 2.11 3D modeling design of the 2nd version prototype (a) Isometric view, (b) Top view	12
Fig. 2.12 3D modeling design of the 3rd version prototype (a) Isometric view, (b) Top view	13
Fig. 2.13 3rd version equipment	14
Fig. 2.14 Specimen bent with constant curvature (a) $R = 100$ mm (b) $R = 80$ mm	15
Fig. 3.1 Flow of the pure bending test	17
Fig. 3.2 Materials for the experiment	18
Fig. 3.3 Moment-curvature diagram for the five materials	21
Fig. 3.4 Tensile tester for tensile test	23
Fig. 3.5 Specimen shape used for tensile test	24
Fig. 3.6 Stress-strain curves of HTPET	25
Fig. 3.7 Stress-strain curves of TPET	25
Fig. 3.8 Stress-strain curves of TLPVC	26
Fig. 3.9 Stress-strain curves of TPPVC	26
Fig. 3.10 Stress-strain curves of ADPET	27
Fig. 3.11 Moment-curvature diagram with regression applied	28
Fig. 3.12 Strain and stress distribution	30
Fig. 3.13 Moment-curvature diagram (Converted from tensile test)	31
Fig. 3.14 Moment-curvature diagram (Tensile test conversion and bending test)	32
Fig. 3.15 Enlarge view of moment-curvature diagram (Tensile test conversion and bending test)	33
Fig. 3.16 Moment-curvature diagram (Single layer and four layers)	34
Fig. 3.17 Moment-curvature diagram with regression applied (Four layers)	35
Fig. 4.1 Pure bending test equipment to be proposed in the future	37

Chapter 1. Introduction

As thin film manufacturing technology develops, products based on existing rigid substrates are changing to flexible next-generation products using flexible substrates that can change shape. Recently, various reports on new transistors [1,2], electronic papers [3,4], organic photovoltaic cells [5,6], batteries [7,8] and display technologies [9,10] having flexibility using various materials and thin film structure manufacturing technologies have appeared. In order to realize these products, it is necessary to structurally reduce the size, thickness and weight of elements entering the product. From a material point of view, it should be possible to transform into various shapes, and a process technology that does not deteriorate in performance even under bending and stretching conditions should be developed.

It is necessary to improve the mechanical reliability problem that occurs in the process of commercialization and mass production of products using thin films or in the driving process. However, since the thin film structure is very thin compared to other structures, it has a behavior different from that of the general bulk structure, and thus, a physical property measurement test different from that of general materials is required. In order to measure the physical and mechanical properties of thin film structures, tensile test that can measure physical properties directly and nanoindentation and bulge tests that can measure physical properties indirectly have been representatively used. From the load-strain curve or pressure-strain curve obtained through these tests, the modulus of elasticity, yield strength, tensile strength, and even Poisson's ratio can be measured. However, thin film structures do not exist alone in the actual use environment, and are laminated on other materials such as substrates to form the structure. In the actual process of forming a laminated structure, residual stress is generated by the interaction between the thin film and the substrate, resulting in bending behavior. The main behavior of flexible, stretchable devices fabricated using such a flexible thin film is bending behavior. Therefore, the main behavior in the process of stacking thin-film structures, the manufacturing process, or the driving process of devices using the thin film structure is the bending behavior [11].

To measure the bending behavior of materials, 3 and 4-point bending test [26-28] and microbeam bending test [29,30] were generally used. The 3 and 4-point bending test is a method that induces pure bending of the specimen through local contact between the pin and the specimen. Through this test, the stress-strain diagram of the material is measured, and as a result, the bending modulus, bending stress, and bending strain can be derived. However, in the case of the 3 or 4-point bending test, a concentrated load is applied through the contact between the pin and the specimen, resulting in an uneven moment along the specimen. In addition, there is a disadvantage that the measurable curvature is limited and does not have a constant curvature along the specimen. The microbeam bending test is a method of applying a cantilever beam test to a specimen through nanoindentation. Through this test, the force and displacement applied to the specimen can be

measured. Recently, atomic force microscopes have made it possible to measure precise material properties in smaller cantilever beams. In the case of the two tests mentioned, a non-uniform moment is applied along the specimen, so the specimen does not actually pure bending, and the measurable radius of curvature is small.

The development of new bending equipment was made to solve the previous problems. Curtis, Wisnom et al., Karakaya [12-14] developed bending test equipment based on two-point bending tests. However, the disadvantage of these devices is that ununiform moments are applied to the specimen and that the specimen does not bend at a constant curvature. Perduijn, Elchalakani, Munoz [15-17] used pulley rotation to induce pure bending on the specimen, but the measurement accuracy was reduced due to pulley-cable interaction, and ununiform moments were applied to the specimen. YOSHIDA et al., Arnold et al. and Boers et al [18-20]. induced pure bending of the specimen through relative motion of the slider and motor. However, the friction of the slider caused an internal force on the specimen. Duncan, Weiss et al., Sanford et al., and Mendiguren et al [21-25]. induced pure bending in the specimen through a four-point bending test method. However, as with the disadvantages of the four-point bending test, the pin caused a concentrated load on the specimen, and the specimen did not have a constant radius of curvature. Most of the experimental equipment described above are test instruments used in sheet metal, so the radius of curvature that can be measured is not large.

Therefore, for thin films that are thinner and more flexible than sheet metals, we intend to design pure bending equipment that can bend the specimen at a constant curvature and have a large radius of curvature that can be measured.

In chapter 2, the design process of the pure bending test equipment for measuring the bending behavior of the thin film has been described. The equipment design process description includes the requirements for applying pure bending to thin films and several prototypes built to meet the requirements.

In chapter 3, The process for verifying the designed pure bending equipment has been described. In order to verify the pure bending equipment, cross-validation was performed through tensile test, and Young's modulus comparison and moment-curvature diagram comparison were performed for verification.

In chapter 4, the conclusions of this study and future works have been described. The conclusions, limitations and expectations that could be obtained by manufacturing pure bending equipment are explained.

Chapter 2. Equipment design

In this chapter, the design process of the pure bending test equipment for measuring the bending behavior of the thin film is described. Through the development of pure bending test equipment, the measurement of flexural rigidity (bending property) in a small curvature range, and the measurement of moment curvature diagram (bending behavior) including large curvature range, are satisfied, and the requirements and design processes for that are shown.

2.1 Requirements for pure bending

In order to measure bending behavior, pure bending must be applied to the specimen. Applying pure bending to thin films in real space is difficult and the implementation of experimental equipment is complicated. Therefore, there are requirements for applying pure bending to the specimen. First, the specimen must have a constant curvature along the specimen, and second, the applied moment along the specimen must be constant. Therefore, the internal force applied to the specimen must be negligibly small compared to the moment applied to the specimen. Therefore, instead of measuring the curvature when pure bending is applied to the thin film, we propose a device that can derive a moment-curvature diagram by measuring the reaction moment when the thin film is bent at a specific curvature.

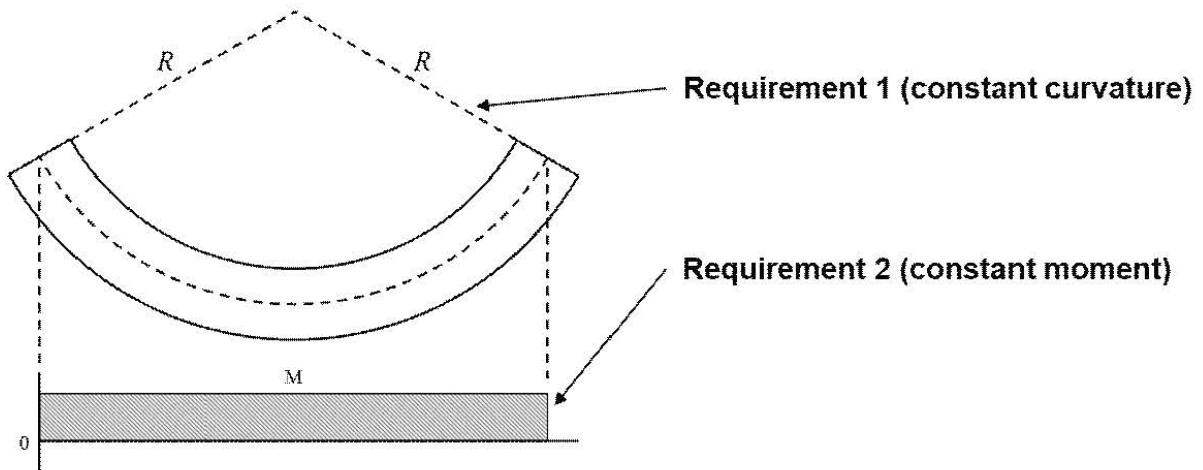


Fig. 2.1 Requirements for pure bending

2.2 Equipment design process

For the design of the experimental equipment, it is necessary to apply a constant moment to the specimen. Therefore, in order to minimize the effect of gravity on the specimen, unlike tests that are generally performed in a horizontal state, the specimen was designed so that the experiment can be performed in a vertical state as shown in Fig. 2.2.

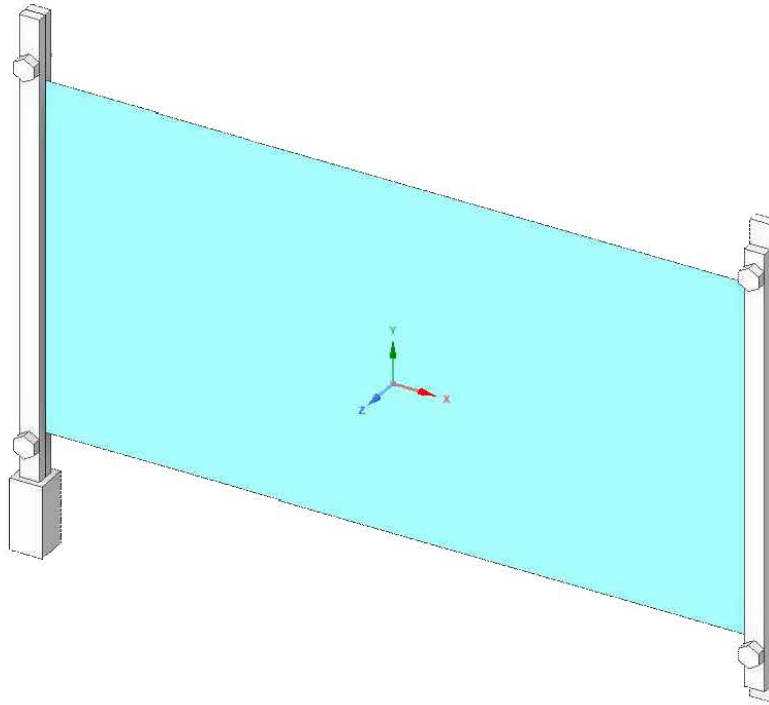


Fig. 2.2 Jigs for fixing the vertical state of the specimen

When pure bending is applied to a specimen, the specimen must be bent with a constant curvature along the specimen. Therefore, when the specimen is bent with a constant curvature, it is necessary to calculate the path at the free end of the specimen, and through this process, the experimental equipment must be manufactured so that the specimen is bent with a constant curvature.

Consider the bending problem of a specimen as shown in Fig. 2.2.

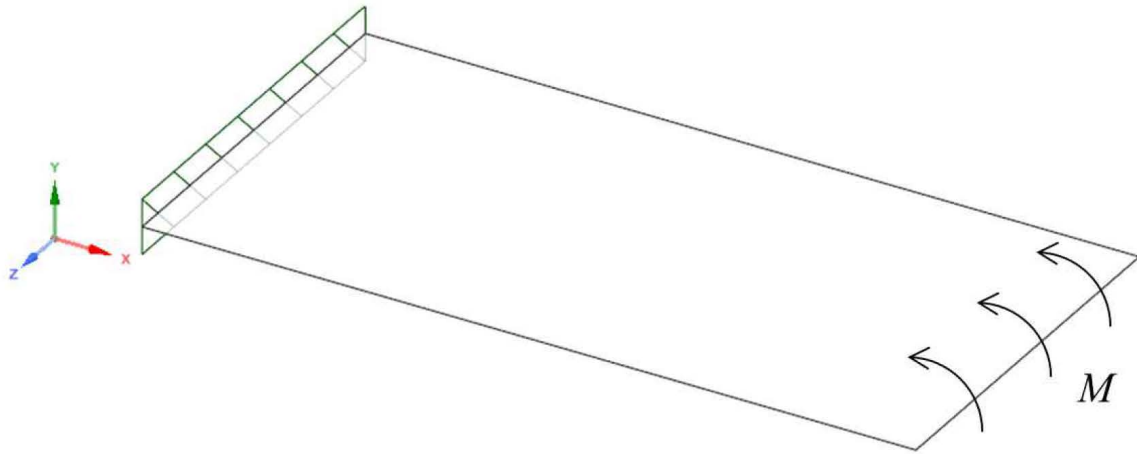


Fig. 2.2 Pure bending of specimen

One end of the thin film is completely fixed, and a bending moment is applied at the free end.

The shape when the specimen is bent at a specific curvature is shown in Fig. 2.3 and Fig. 2.4

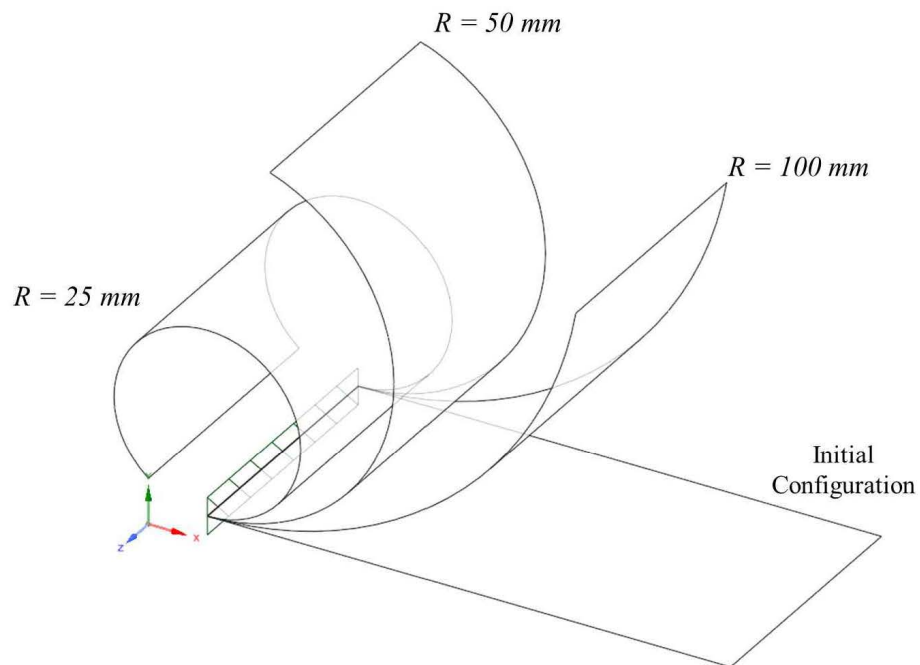


Fig. 2.3 Deformed shapes of specimen

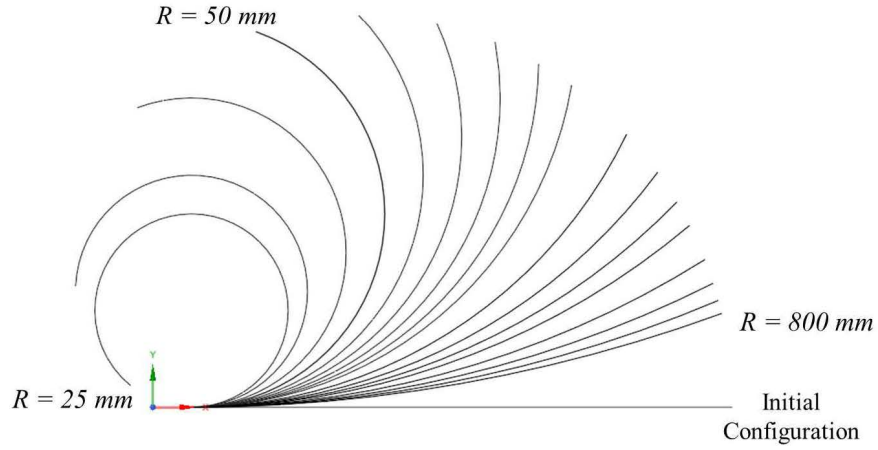


Fig. 2.4 Deformed shapes of specimen in XY Plane

In order to change the curvature while maintaining the length of the arc, it is necessary to know the information about the X, Y coordinates of the free end and the central angle of the arc [31]. For the X, Y coordinates of the free end and the central angle of the arc, the function of the central angle theta shown in Fig. 2.5 is as follows,

$$\kappa = \frac{1}{R} = \frac{\theta}{L}, \quad (2.1)$$

$$x(\theta) = L \frac{\sin \theta}{\theta}, \quad (2.2)$$

$$y(\theta) = L \frac{(1 - \cos(\theta))}{\theta}, \quad (2.3)$$

where L is length of the thin film, and θ is the domain of the function of curvature and the X, Y coordinates of the free end of the thin film, can also be referred to as the central angle of an arc in the form of a thin film, but the angle θ is defined as the angle between the tangent to the tip of the moving thin film and the X axis.

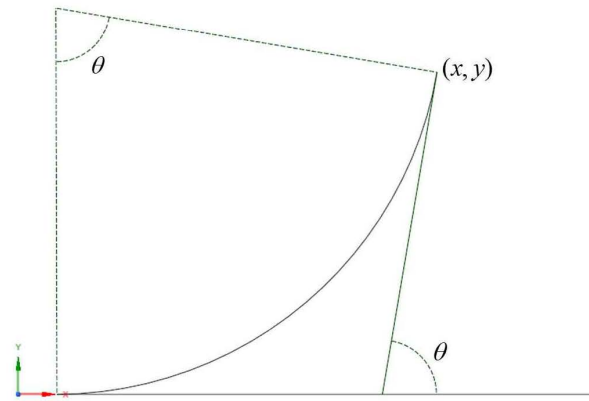


Fig. 2.5 Definition of displacement and theta of thin film when the specimen is bent

When length of the thin film is 140 mm, the shape of the thin film (blue line) satisfying Eqs. (2.1) to (2.3) and the trace of the free end of the thin film (red line) are shown in Fig. 2.6.

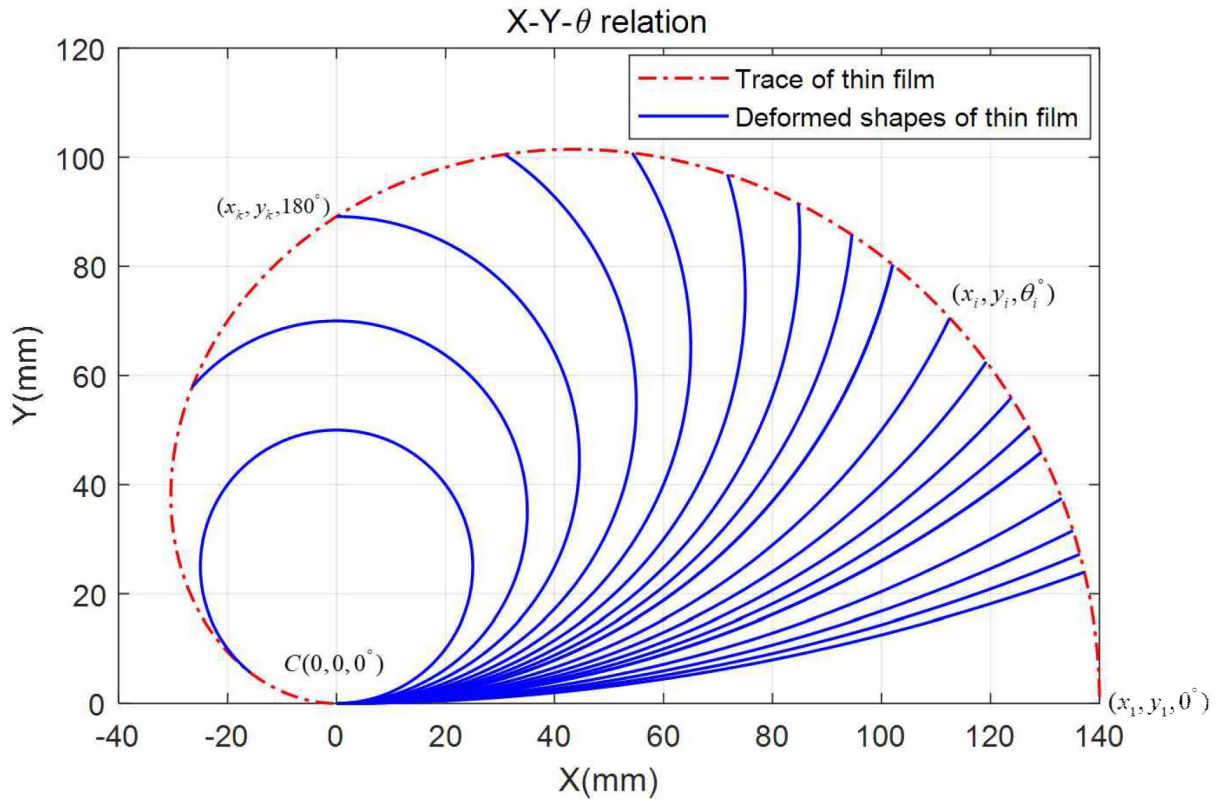
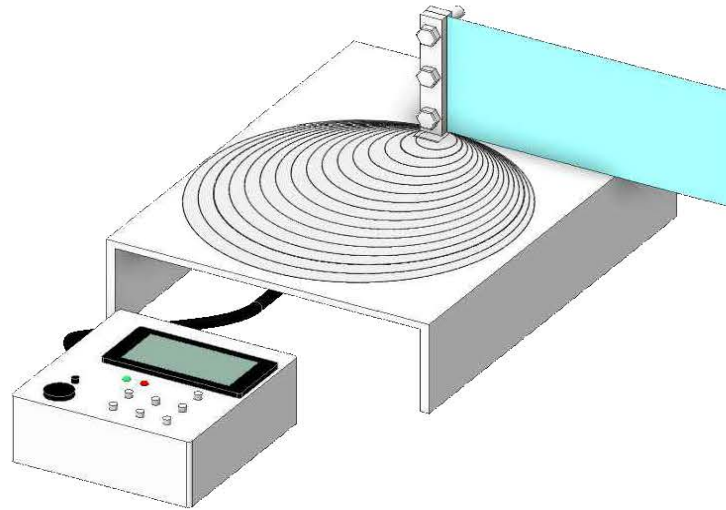
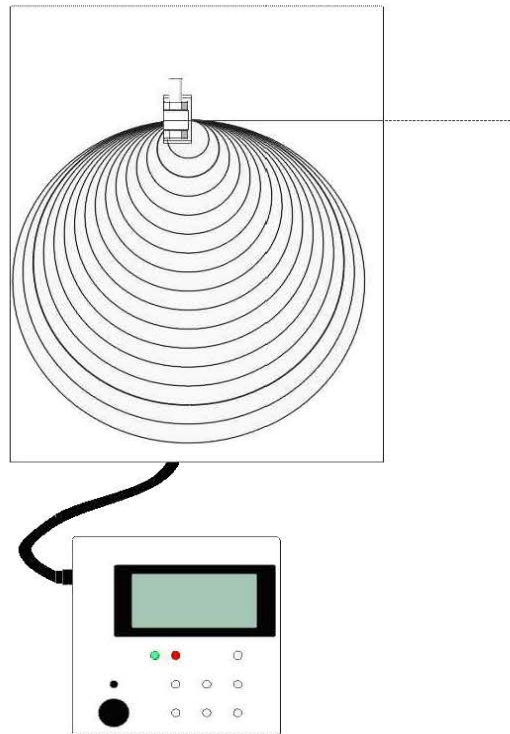


Fig. 2.6 Deformed shapes and trace of of the free end of the thin film when the thin film is bent

Based on the requirements including chapter 2.2, the first prototypes shown in Fig. 2.7 and Fig. 2.8 were produced.



(a)



(b)

Fig. 2.7 3D modeling design of the 1st version prototype (a) Isometric view, (b) Top view

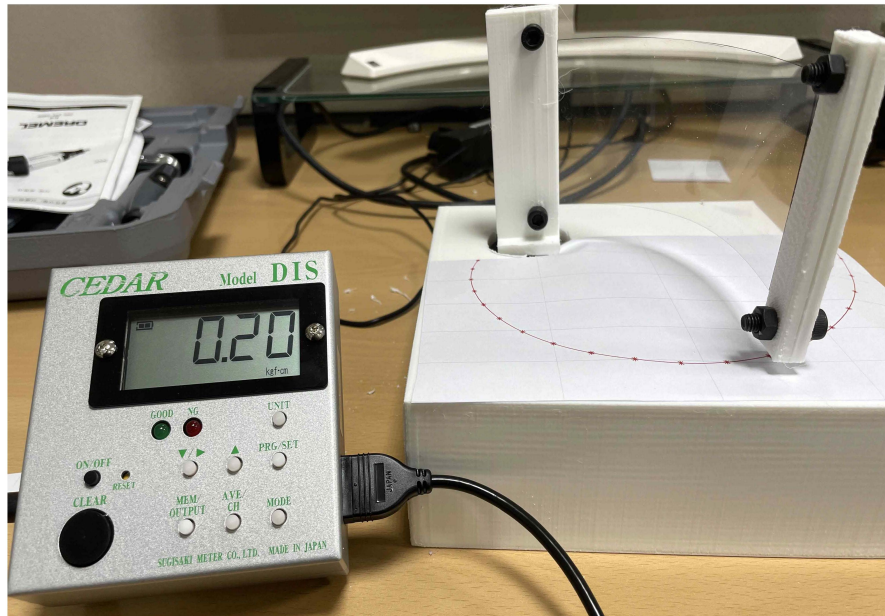


Fig. 2.8 1st version equipment

In the case of the 1st version prototype, the free end of the specimen can be moved to the desired X, Y coordinates, but the jig angle at the free end of the specimen cannot be fixed, so there is a problem that internal force is applied to the specimen.

Therefore, in order to minimize the internal force applied to the specimen by the angle of the jig at the free end of the specimen, holes through which the jig can enter were drilled in the support plate as shown in Fig. 2.9 and Fig. 2.10. These holes are drilled perpendicular to the free end of the specimen to minimize the internal force applied to the specimen.

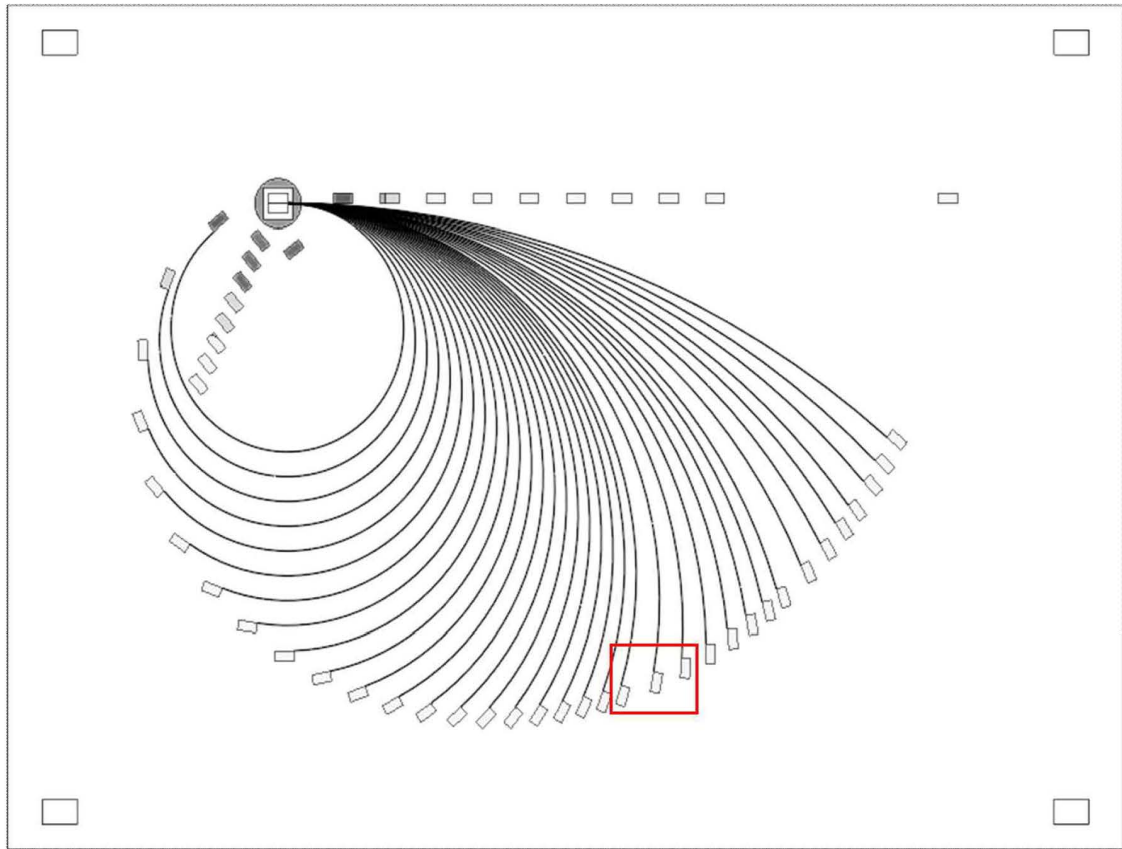


Fig. 2.9 Arc and jig holes (Top view)

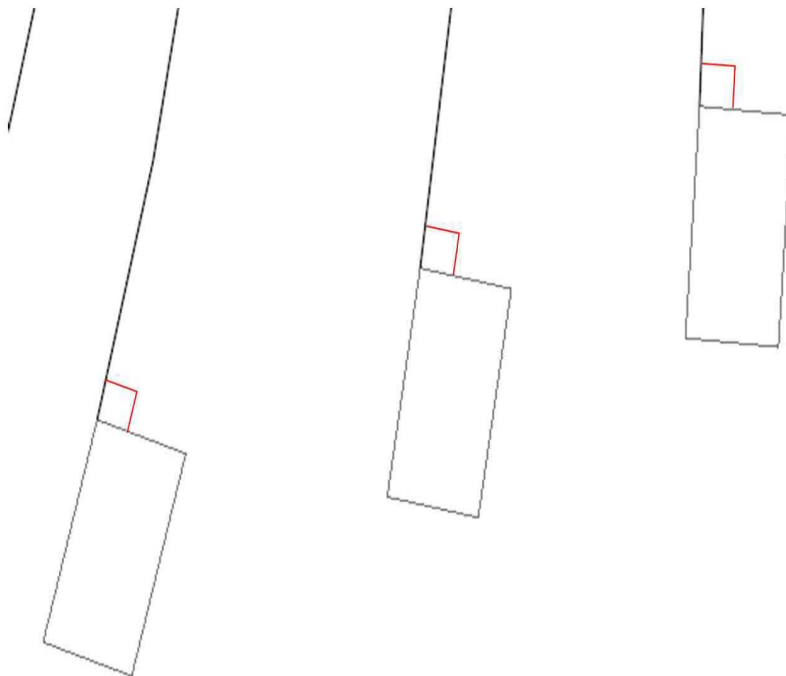
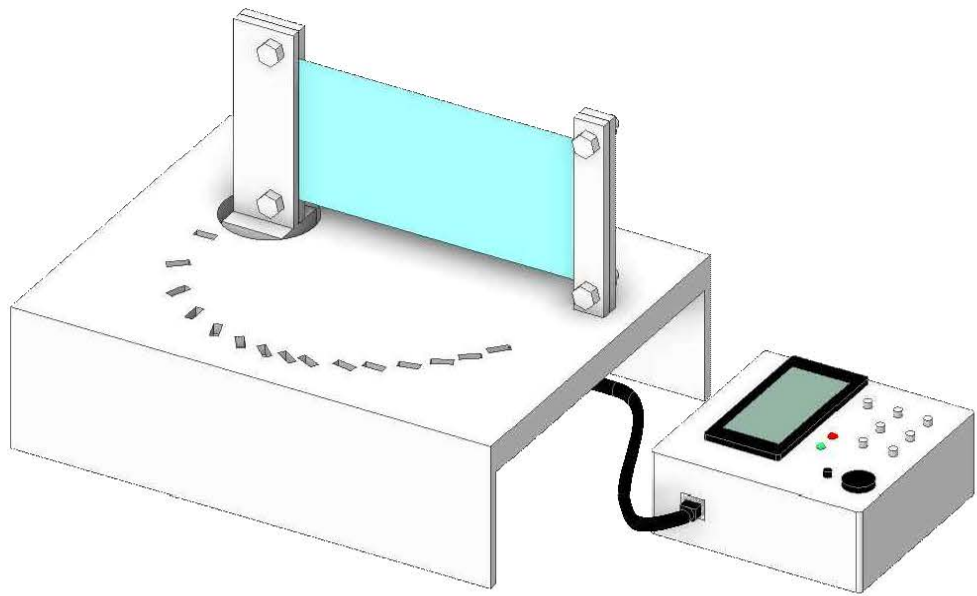
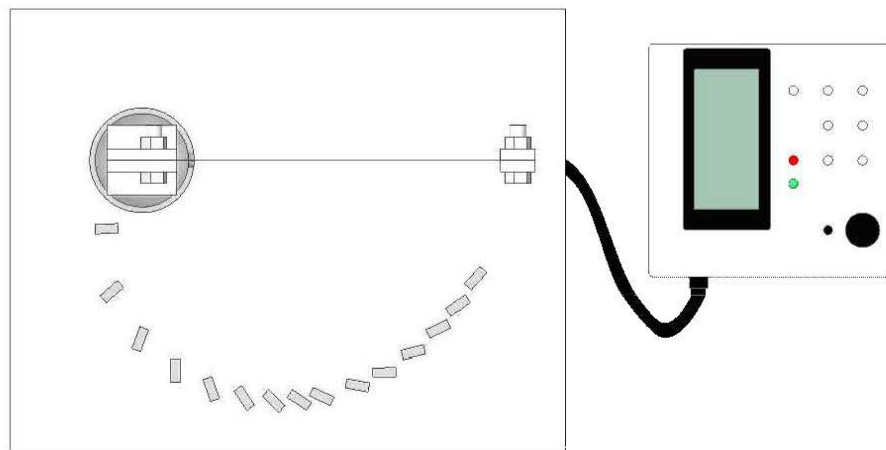


Fig. 2.10 Arc and jig holes (Enlarge view)

The 2nd version prototype was designed as shown in Fig. 2.11 by drilling a hole in the support plate for the jig to fit through. In the case of the 2nd version prototype, the angle formed by the tangential line of the thin film and the X-axis can be adjusted so that the central angle of the arc formed by the thin film is the same as that of the first prototype. However, in the process of measuring the moment of the specimen, the free end jig was not fixed vertically and was tilted. Also, the width of the jig was too thick to make an arc of larger curvatures. In order to solve these two problems, a plate was additionally designed at the top of the jig to fix the jig to the free end. (See Fig. 2.12 and Fig. 2.13)

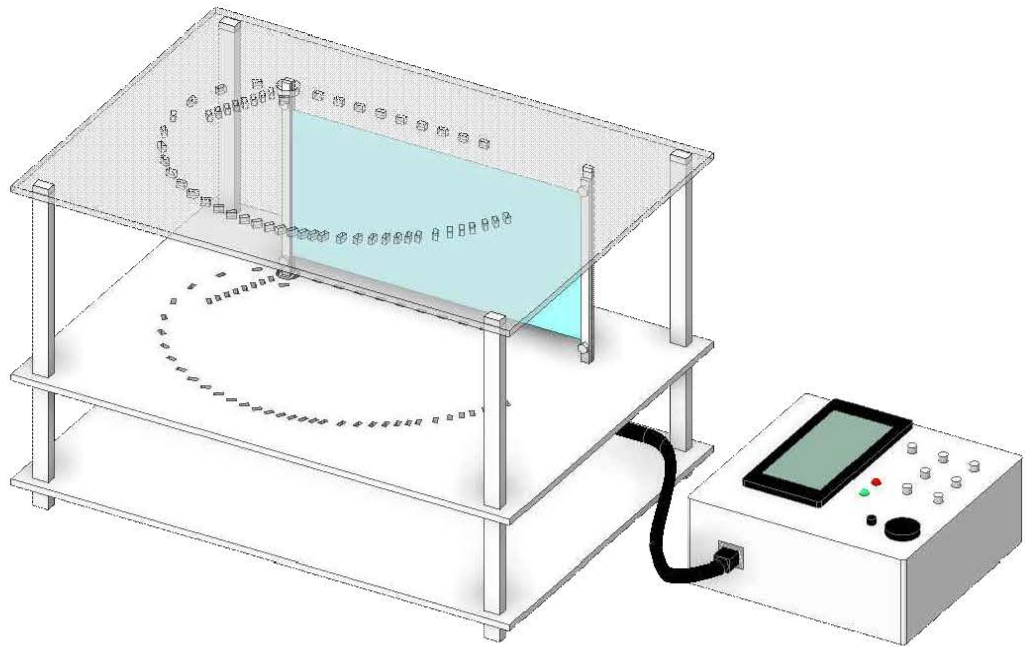


(a)

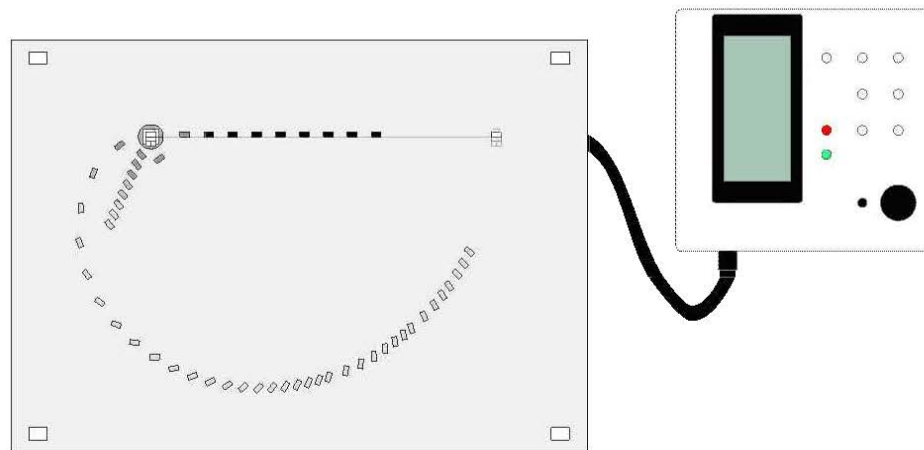


(b)

Fig. 2.11 3D modeling design of the 2nd version prototype (a) Isometric view, (b) Top view

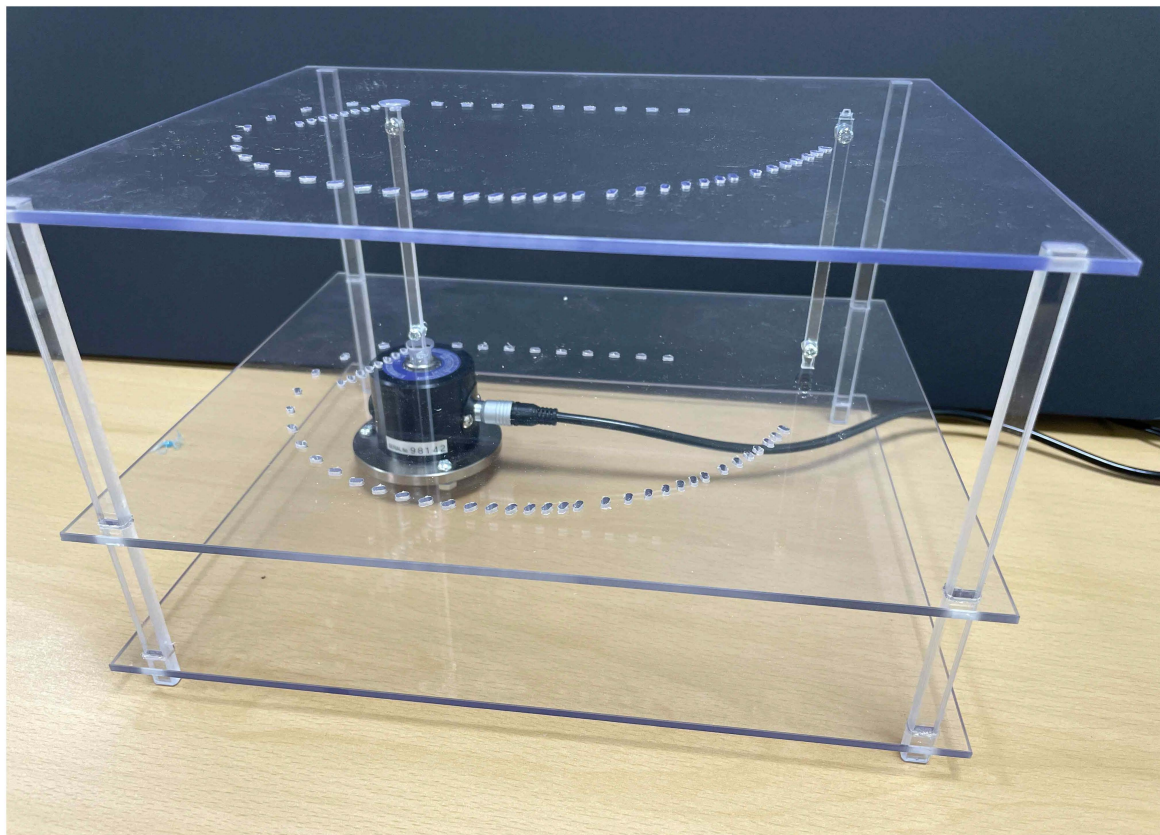


(a)

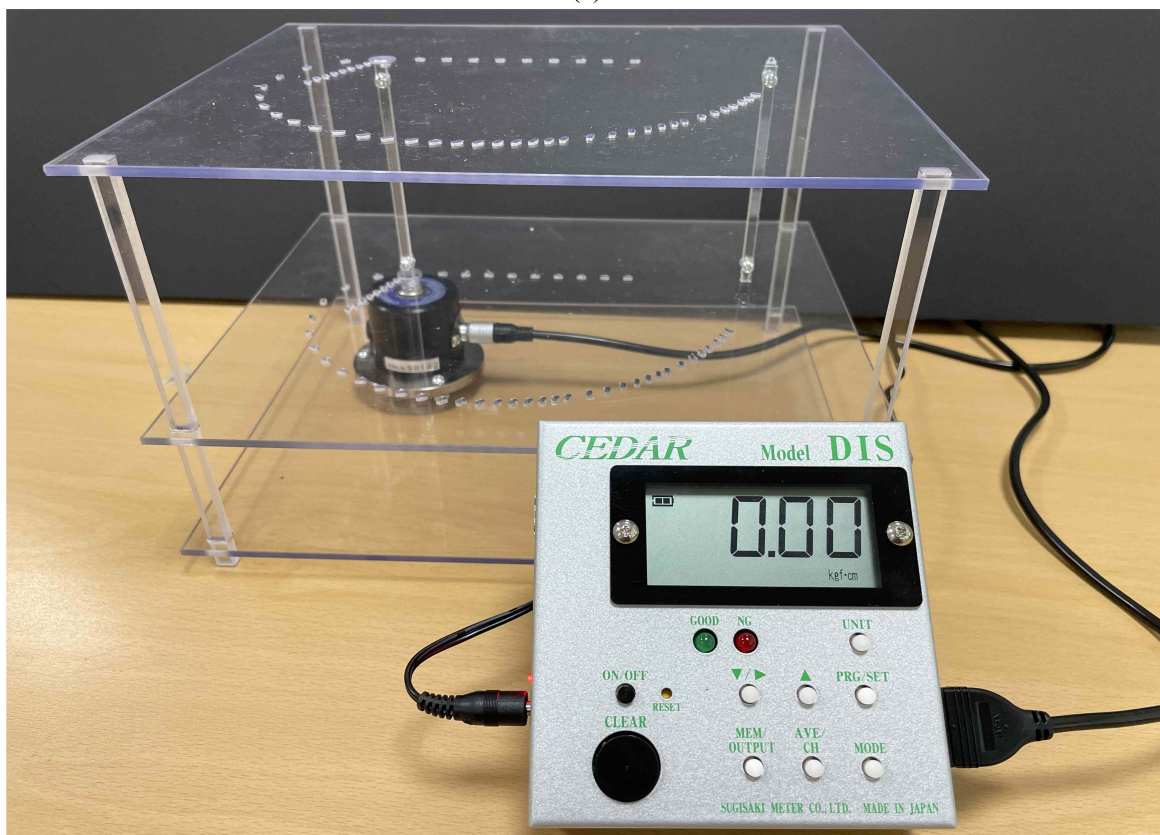


(b)

Fig. 2.12 3D modeling design of the 3rd version prototype (a) Isometric view, (b) Top view



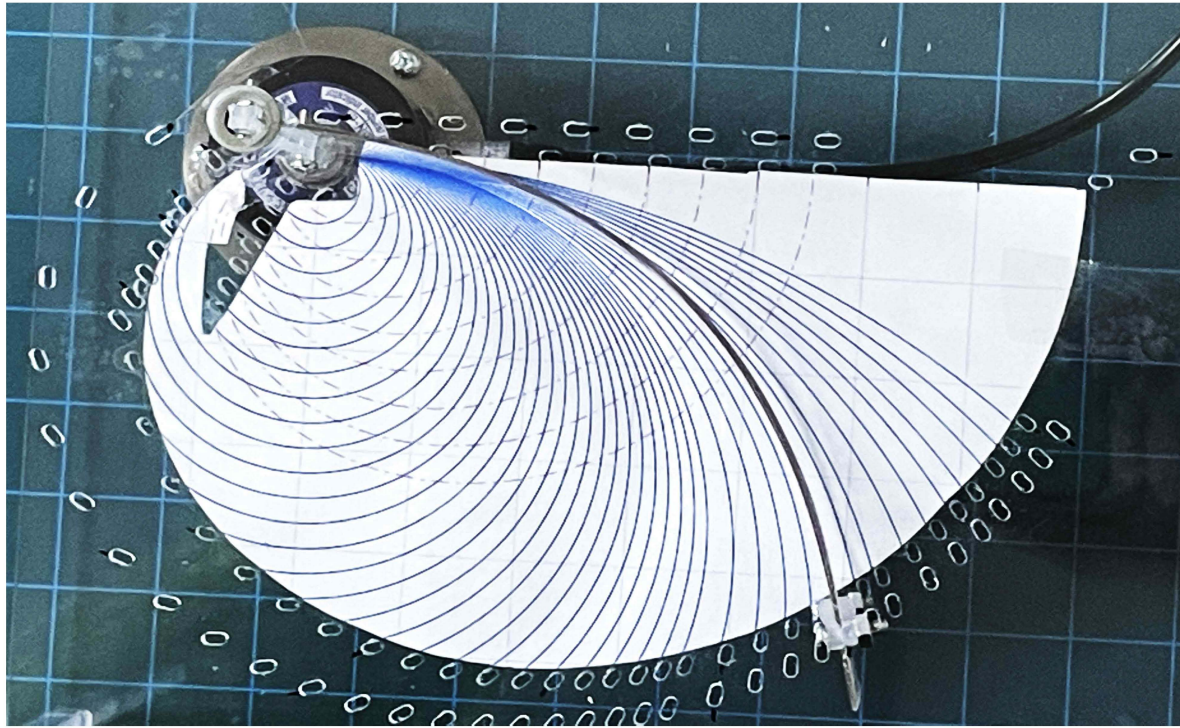
(a)



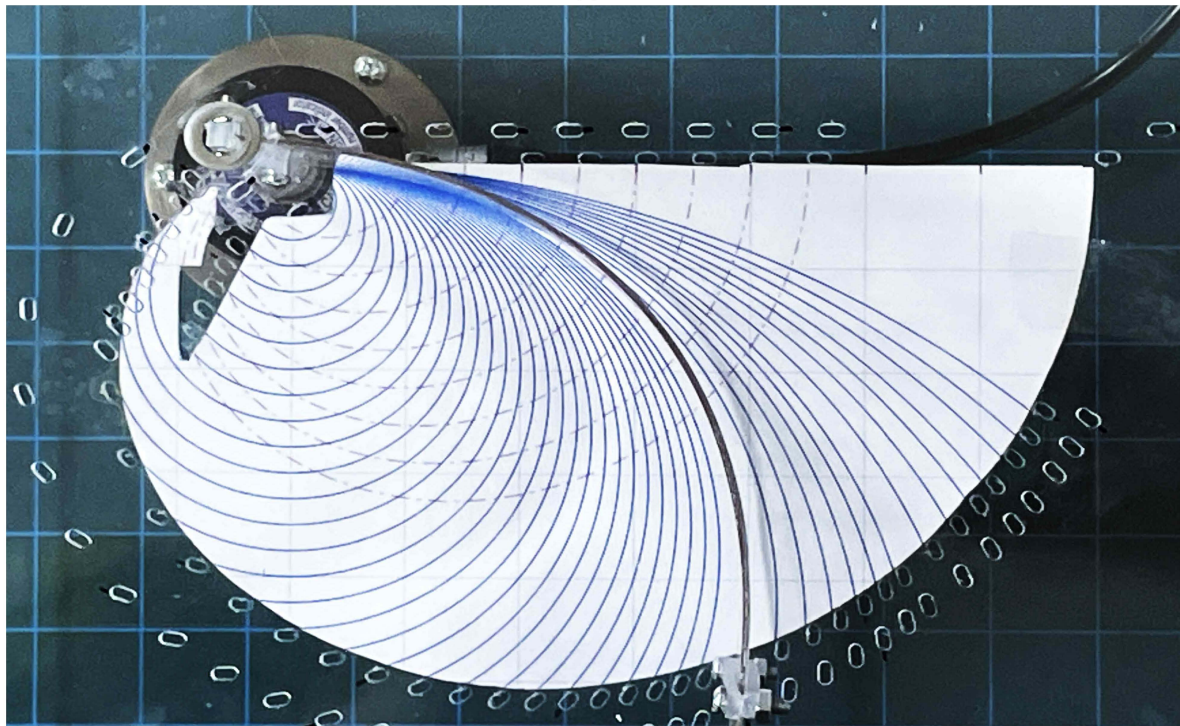
(b)

Fig. 2.13 3rd version equipment

As a result of the additional design with a plate on top of the jig, the specimen could be bent to the desired curvature as shown in Fig. 2.14 and had a constant curvature along the specimen.



(a)

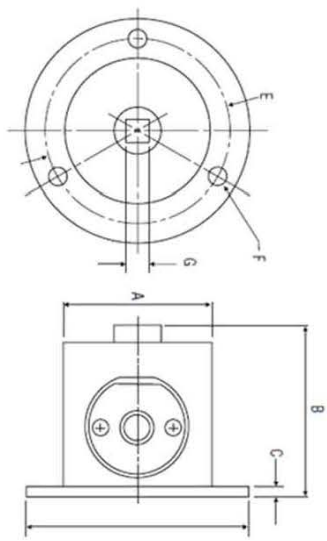


(b)

Fig. 2.14 Specimen bent with constant curvature (a) $R = 100$ mm (b) $R = 80$ mm

Finally, a torque meter was used to measure the reaction moment when the fixed end was bent with a specific curvature, and the specifications of the torque meter used in the design of the experimental equipment are as follows.

Table 2.1 Torque Meter Specification

Model			DIS-IP5
Measurement range			0.020 ~ 5 N·m
			0.20 ~ 50 kgf · cm
			0.20 ~ 45 lbf · in
Accuracy			± 0.5 %
Detector Outside dimension	A	φ 40	
	B	41.2	
	C	5	
	D	φ 60	
	E	φ 50	
	F(P.C.D)	φ 4.2	
	G(Plug form)	6.35 sq	
	Weight(g)	200 g	

Through the design of the experimental equipment, the following conditions were satisfied.

1. It is possible to apply pure bending to the specimen.
2. The specimen can be bent to the desired curvature.
3. When a specimen is bent in an arc shape, the corresponding reaction moment can be measured.

Chapter 3. Experimental verification

In this chapter, an experimental validation process is described to ensure the reliability of a pure bending test rig designed to measure the bending behavior of specimens. A pure bending test was performed with an experimental equipment designed to verify the pure bending test equipment, and a tensile test was performed with a tensile tester to compare the results.

3.1 Pure bending test

As explained in Chap. 2.1, in order to satisfy requirements 1 and 2, a method of fixing the thin film at a specific curvature was used instead of applying a pure moment to the thin film. In addition, a torque meter was used to measure the reaction moment the fixed end when it was bent at a specific curvature.

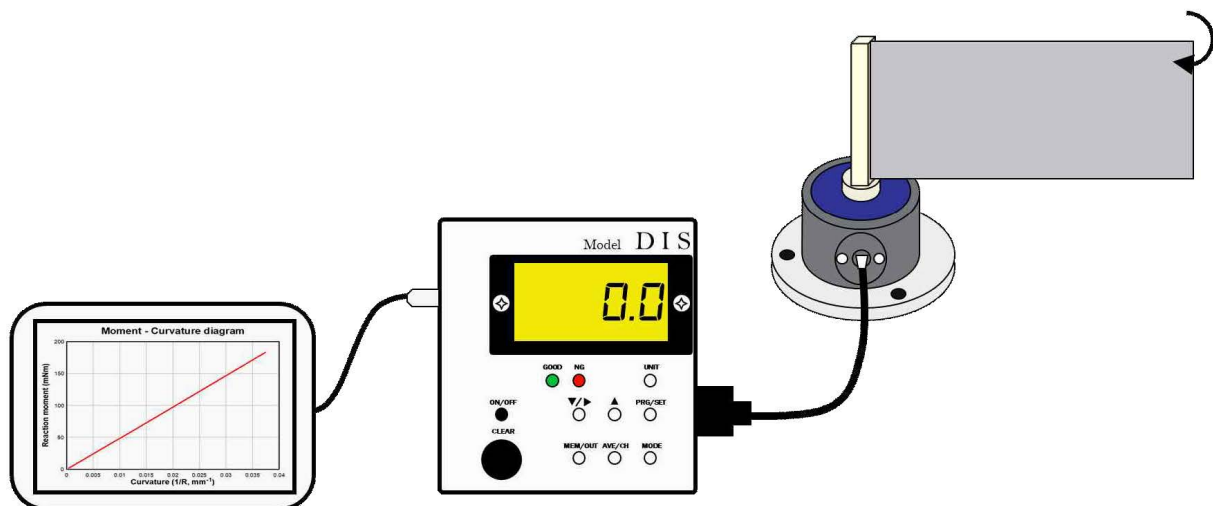


Fig. 3.1 Flow of the pure bending test

The flow of the pure bending test based on this is shown in Fig. 3.1. The order of the test is as follows.

1. Insert the jig into the joint of the torque meter and fix the specimen to the jig.
2. Record the reaction moment measured by the torque meter when the specimen is bent to a specific curvature.
3. Plot the moment curvature diagram with measured moment for each curvature.
4. Calculate the flexural rigidity, which is the mechanical bending property of the specimen.

The experiment was conducted with the experimental equipment shown in Fig. 2.13 shown in chapter 2, and the materials used are shown in Fig. 3.2.

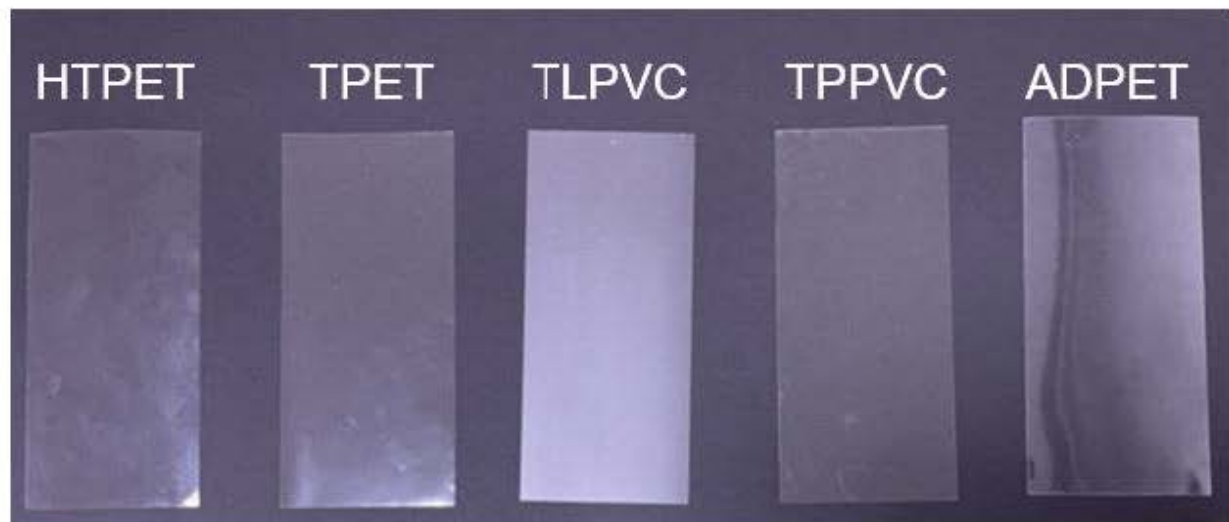
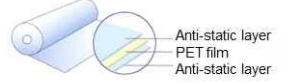



Fig. 3.2 Materials for the experiment

The five materials shown in Fig. 3.2 and Table 3.1 are:

1. Highly transparent PET film(HTPET),
2. Transparent PET film(TPET),
3. Translucent PVC film(TLPVC),
4. Transparent PVC film(TPPVC),
5. Adhesive transparent PET film(ADPET).

Table 3.1 Materials for the experiment

Material	# of layers	Etc.	
HTPET (Highly transparent PET film)	3	2 antistatic layer exists	
TPET (Transparent PET film)	1		
TLPVC (Translucent PVC film)	1	Translucent	
TPPVC (Transparent PVC film)	1		
ADPET (Adhesive transparent PET film)	2	1 release film exists	

The results obtained from the pure bending test shown in Fig. 2.14 using the pure bending test equipment shown in Fig. 2.13 are shown in Tables 3.2 and 3.3.

Table 3.2 Results for each material (Unit: kgf·cm)

Radius (mm)	Arc length (mm ⁻¹)	Curvature (mm ⁻¹)	Moment (kgf·cm)				
			HTPET	TPET	TLPVC	TPPVC	ADPET
4	10	0.25	0.005	0.005	Yl*	Yl*	0.045
5	20	0.2	-	-	Yl*	Yl*	0.035
10	40	0.1	-	-	0.165	0.085	0.02
12.5	50	0.08	-	-	0.135	0.07	-
20	80	0.05	-	-	0.09	0.045	-
25	140	0.04	-	-	0.075	0.035	-
40	140	0.025	-	-	0.045	0.03	-
50	140	0.02	-	-	0.04	0.02	-
62.5	140	0.016	-	-	0.025	-	-
80	140	0.0125	-	-	0.02	-	-

Table 3.3 Results for each material (Unit: N·mm)

Radius (mm)	Arc length (mm ⁻¹)	Curvature (mm ⁻¹)	Moment (N·mm)				
			HTPET	TPET	TLPVC	TPPVC	ADPET
4	10	0.25	0.49035	0.49035	YI*	YI*	4.41315
5	20	0.2	-	-	YI*	YI*	3.43245
10	40	0.1	-	-	16.18155	8.33595	1.9614
12.5	50	0.08	-	-	13.23945	6.8649	-
20	80	0.05	-	-	8.8263	4.41315	-
25	140	0.04	-	-	7.35525	3.43245	-
40	140	0.025	-	-	4.41315	2.9421	-
50	140	0.02	-	-	3.9228	1.9614	-
62.5	140	0.016	-	-	2.45175	-	-
80	140	0.0125	-	-	1.9614	-	-

Tables 3.2 and 3.3 show "-" and "YI", where "-" is not measured because the moment applied to the fixed end is small and the torque meter is not within the measurable range. In the case of "YI", a yard line occurs in the specimen before fixing the jig of the specimen free end. The reaction moment was measured in kgf·cm (see Table 3.2) and converted into N·mm (see Table 3.3)

Fig. 3.3 shows the results of the moment curvature diagram showing the measured reaction moment for each curvature for the five materials shown in Table 3.3.

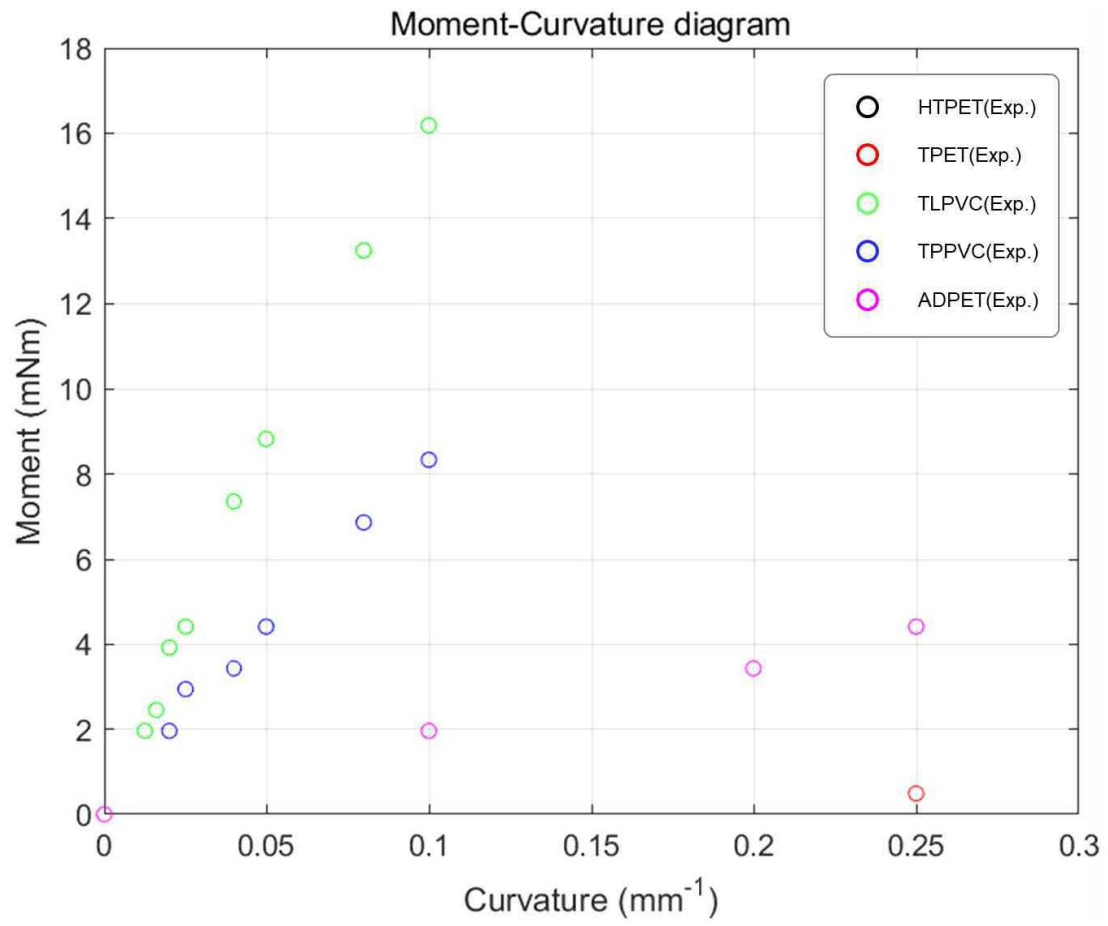
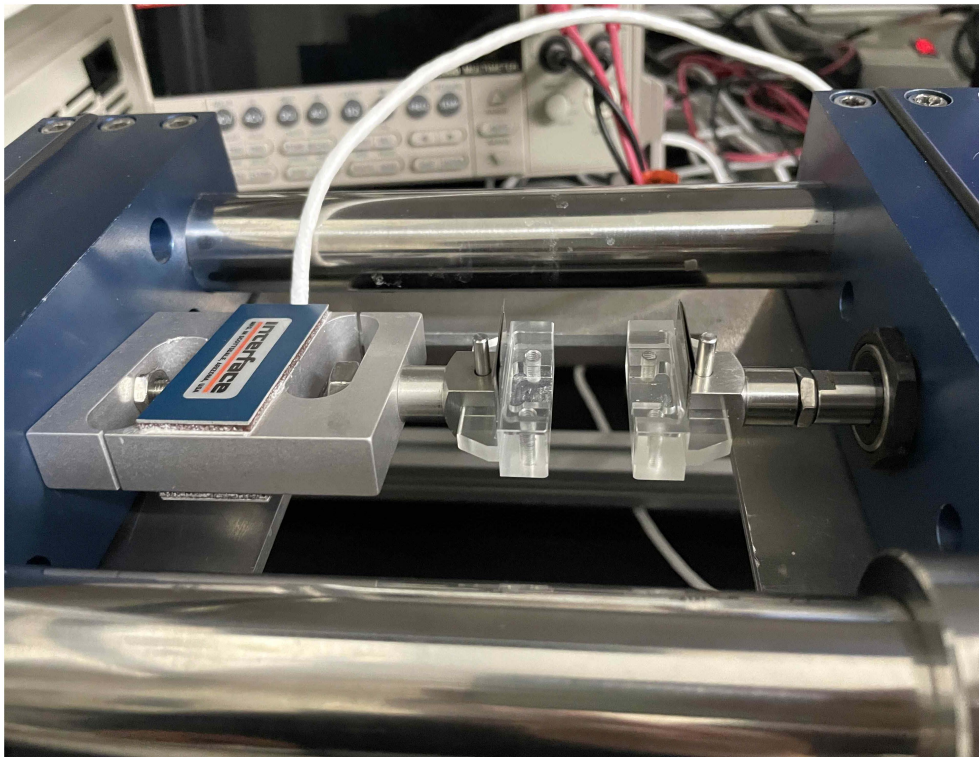


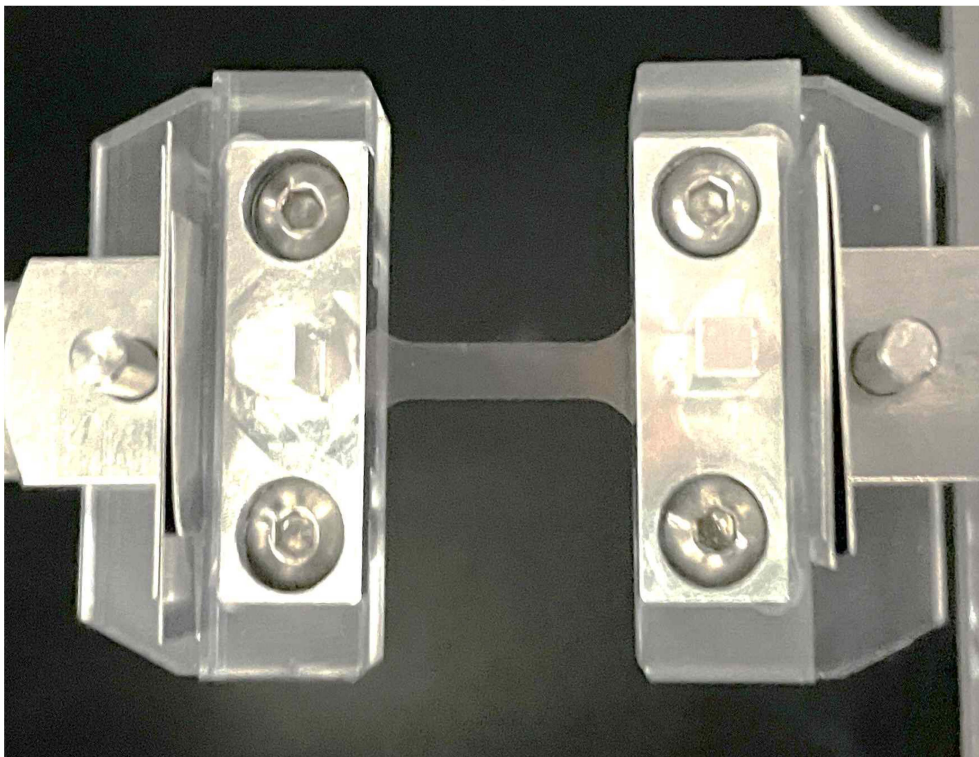
Fig. 3.3 Moment-curvature diagram for the five materials

3.2 Tensile test

To verify the designed pure bending test equipment and to verify the anisotropy of the material, the tensile test was performed with the tensile tester shown in Fig. 3.4. And Fig. 3.5 shows the shape of the specimen used for the tensile test.



(a)



(b)

Fig. 3.4 Tensile tester for tensile test

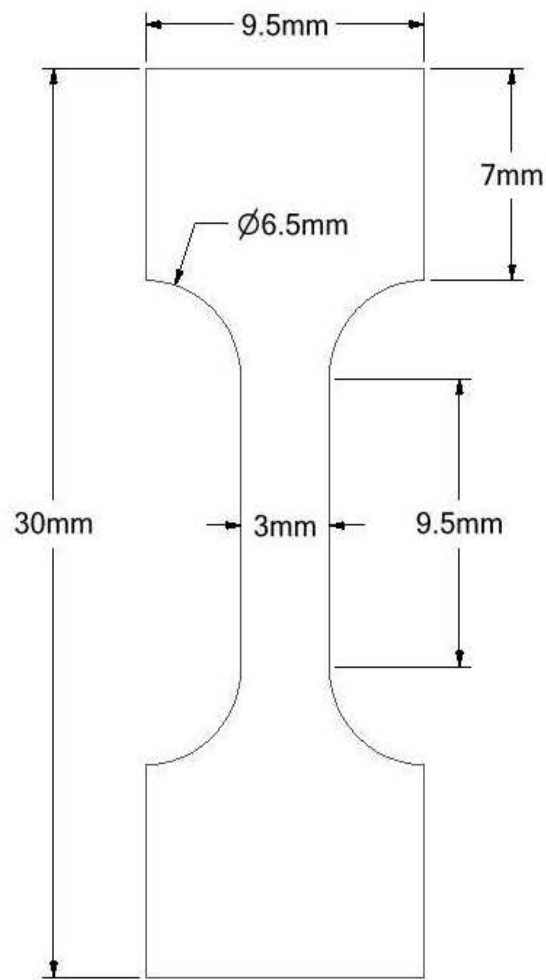


Fig. 3.5 Specimen shape used for tensile test

The tensile test was performed on five materials, and three times per direction were performed on two perpendicular directions. The stress-strain curve for each material and direction obtained through the tensile test is shown in the following figures.

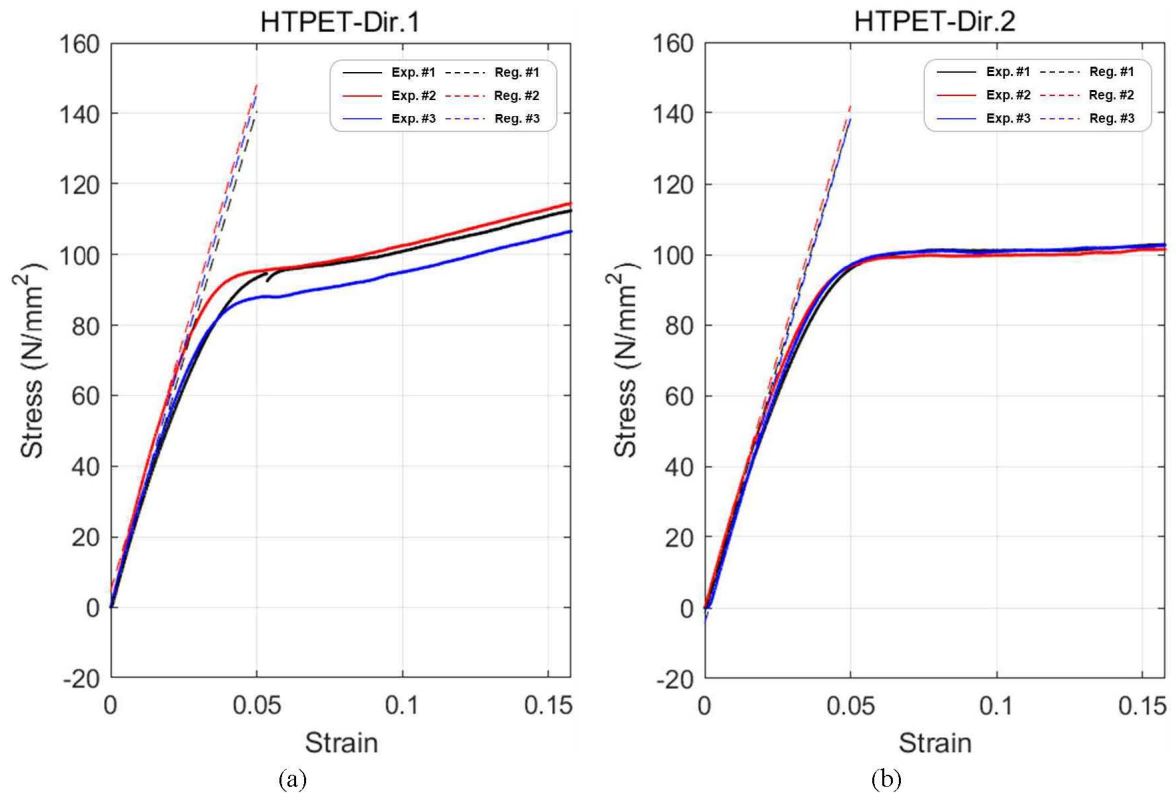


Fig. 3.6 Stress-strain curves of HTPET

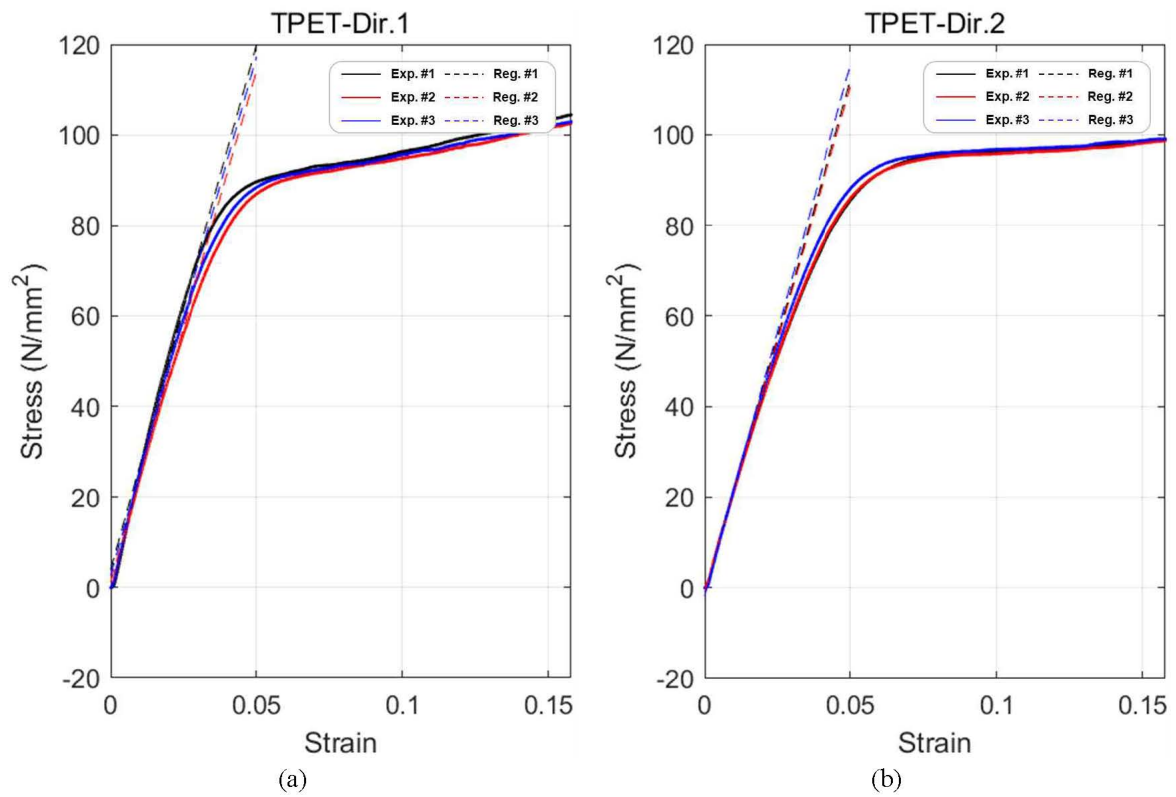


Fig. 3.7 Stress-strain curves of TPET

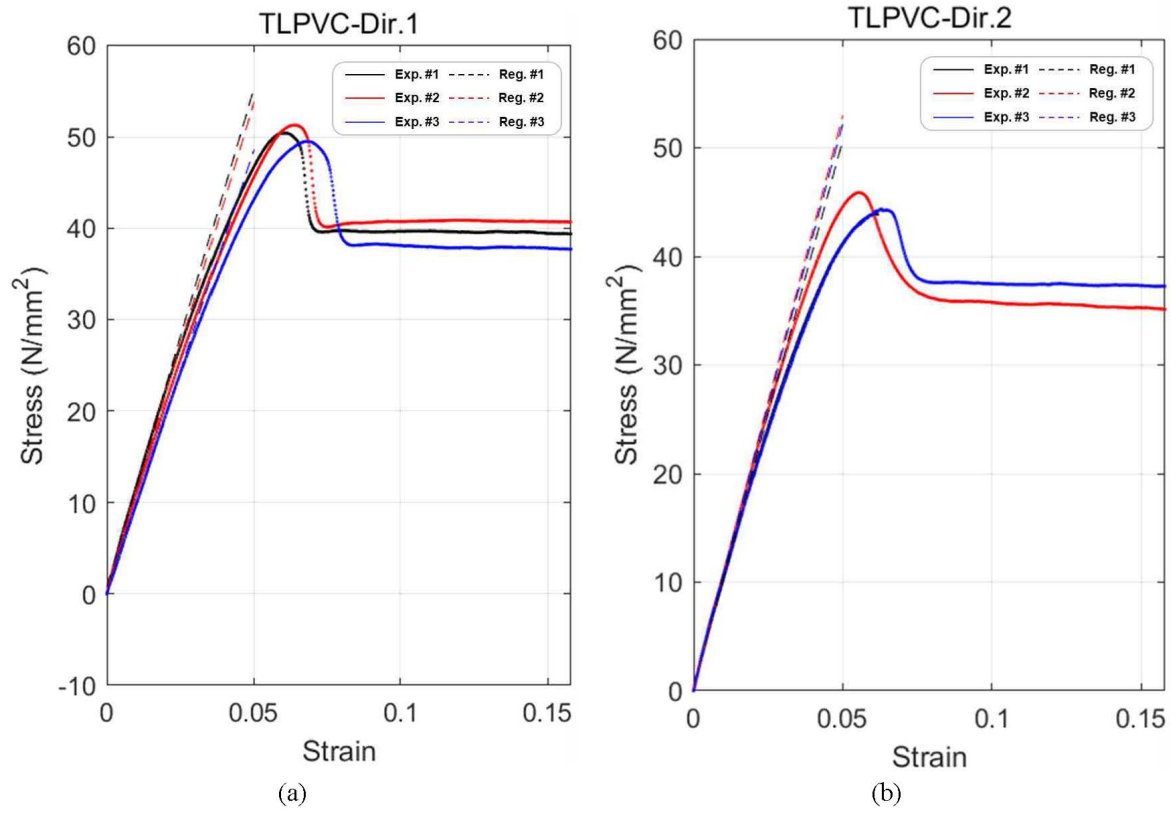


Fig. 3.8 Stress-strain curves of TLPVC

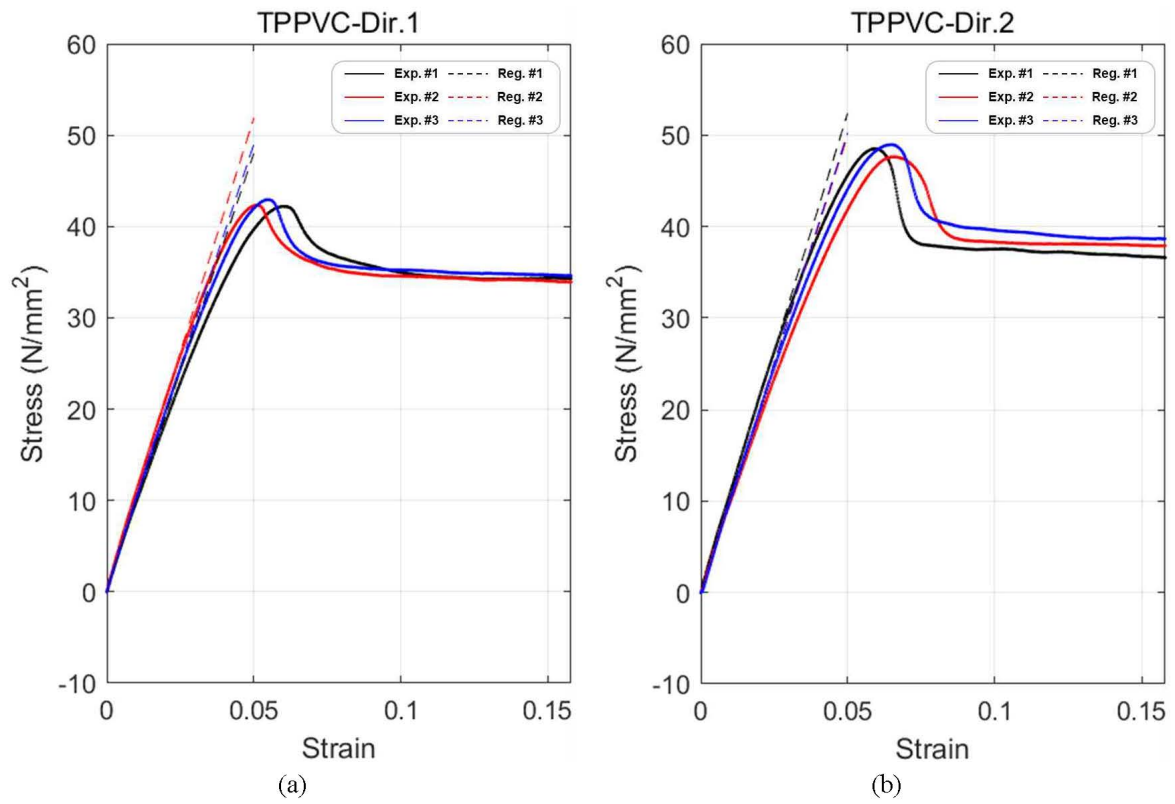


Fig. 3.9 Stress-strain curves of TPPVC

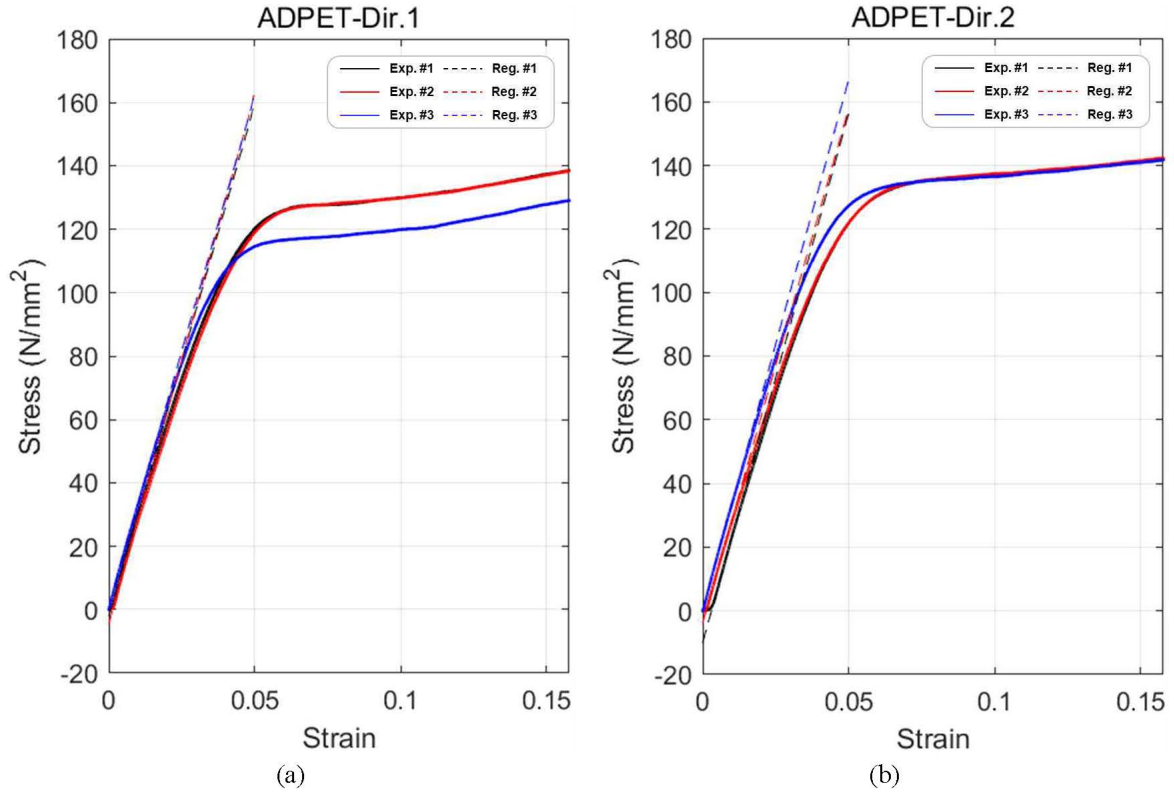


Fig. 3.10 Stress-strain curves of ADPET

The dotted lines shown in Figs. 3.6 to 3.10 are the results of linear regression in the part where the strain is small to obtain the mechanical properties from the stress-strain curve. The mechanical properties of the five materials derived through linear regression are shown in Table 3.4.

Table 3.4: Mechanical properties for the experiment

Material	ν	$t(mm)$	$E_1(MPa)$	$E_2(MPa)$
HTPET	0.43	0.05	2865	2838
TPET	0.43	0.05	2290	2278
TLPVC	0.4	0.3	4043	1032
TPPVC	0.4	0.26	992	1013
ADPET	0.43	0.075	3272	3299

Through the Young's modulus for each direction shown in Table 3.4, it can be assumed that all materials used in the experiment are isotropic materials.

3.3 Young's modulus comparison

The first verification of the pure bending experimental equipment manufactured by comparing the Young's modulus directly obtained in the tensile test and the Young's modulus indirectly obtained in the bending test was performed. By applying regression to the moment-curvature data obtained from the bending test, flexural rigidity was obtained from the slope value in the range of small curvature, and Young's modulus was derived from the flexural rigidity of each obtained material.

The moment-curvature diagram shown based on the results of Table 3.3 to which regression analysis is applied is shown in Fig. 3.11. The regression model of the moment-curvature diagram of Fig. 3.3 is shown in Table 3.5.

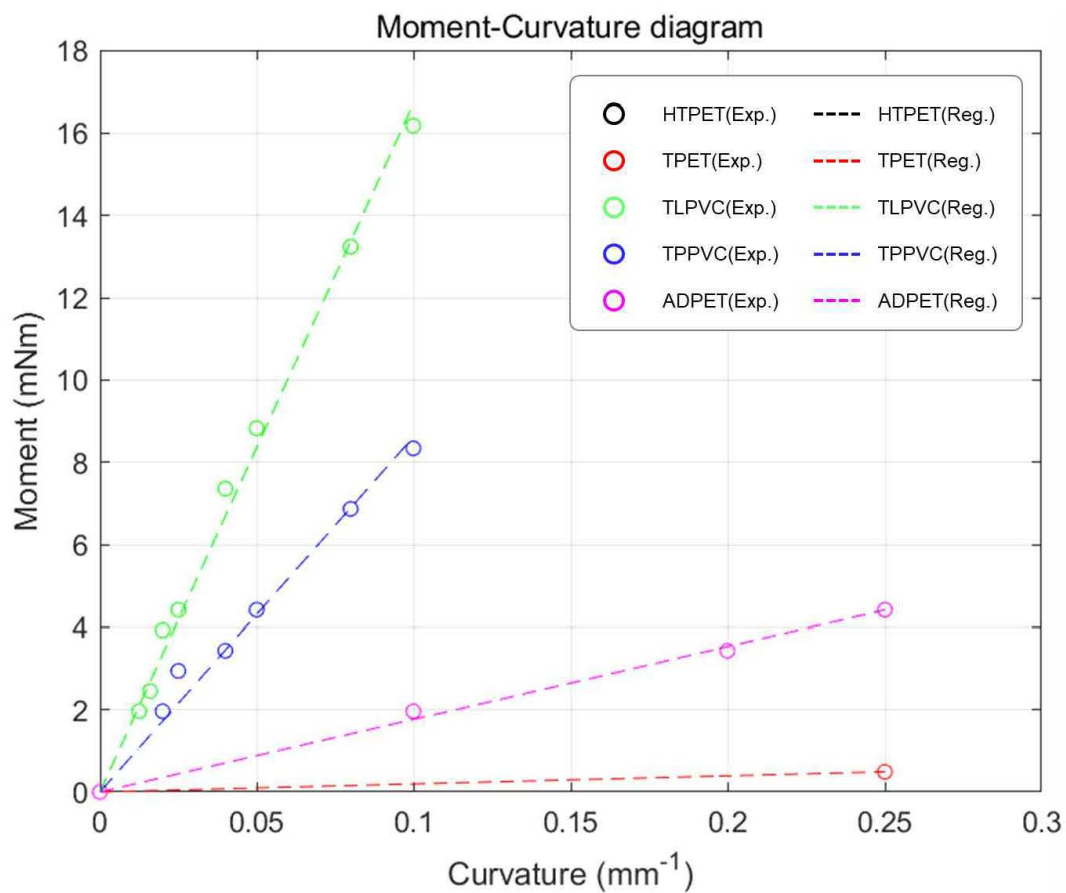


Fig. 3.11 Moment-curvature diagram with regression applied

Table 3.5 Regression results for each material

Material	Regression Model $f(x) = ax$	Flexural rigidity (N·mm)
HTPET	$f(x) = 1.961x$	0.028014
TPET	$f(x) = 1.961x$	0.028014
TLPVC	$f(x) = 167.1x$	2.3871
TPPVC	$f(x) = 86.11x$	1.2301
ADPET	$f(x) = 17.65x$	0.25214

Table 3.5 also shows the flexural rigidity calculated by dividing the slope of the linear regression model by the width of each specimen. Based on the flexural rigidity shown in Table 3.5, the results of comparing the Young's modulus of each material obtained according to the thin plate theory [32] and the Young's modulus obtained through a tensile test are shown in Table 3.6.

Table 3.6 Results of Young's modulus comparison

Material	Flexural rigidity (N·mm)	Young's modulus (MPa) (bending)	Young's modulus (MPa) (tensile)	Difference (%)
HTPET	0.028014	2686.371	2851.5	-5.67
TPET	0.028014	2686.371	2284	17.75
TLPVC	2.3871	1060.952	1037.5	2.26
TPPVC	1.2301	1067.832	1002.5	6.52
ADPET	0.25214	3025.714	3285.5	-7.91

Comparing the Young's modulus obtained through pure bending and tensile tests, the difference between the two values was less than 10% for the remaining four materials except for TPET. Verification of pure bending test equipment through Young's modulus comparison can be said to be reliable to some extent.

3.4 Moment-curvature diagram comparison

The second verification of the pure bending experimental equipment manufactured through the comparison of the moment-curvature diagram was performed. Comparing the result data of the bending test and the tensile test, the number of data of the tensile test is higher than that of the bending test. Therefore, instead of converting the moment-curvature data obtained in the bending test into stress-strain data, it went through a process of converting the stress-strain data obtained in the tensile test into moment-curvature data.

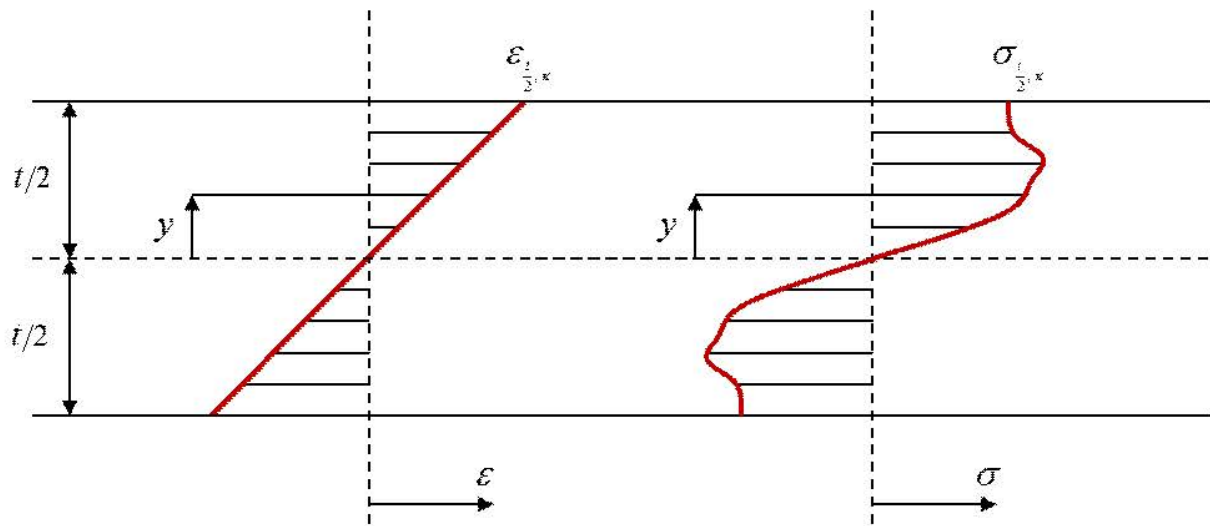


Fig. 3.12 Strain and stress distribution

The strain and stress distribution in the thickness direction when pure bending is applied to the specimen are shown in Fig. 3.12 [33]. It was assumed that the strain in the thickness direction was proportional to the distance from the neutral axis. The maximum strain when the specimen is bent at a specific curvature can then be obtained and converted from stress-strain data to moment-strain data because the stress distribution is known. The results obtained from the tensile test performed in chapter 3.2 were used for the data of the strain and stress used for the conversion.

As shown in Fig. 3.12, considering the stress distribution of the specimen cross section with unit width when bending, the moment applied to the specimen cross section can be obtained by integrating the stress applied to the cross section as shown in the following Eq, (3.1).

$$M(y) = \int_{-t/2}^{t/2} y\sigma(y)dy = \frac{2}{K^2} \int_0^{\varepsilon_{t/2,K}} \varepsilon\sigma(\varepsilon)d\varepsilon \quad (\because \varepsilon = yK), \quad (3.1)$$

Since the stress-strain rate data obtained by the tensile test are numerical data, the following Eq. (3.2) is used when transformed into a numerical integral,

$$M(y) = \frac{1}{K^2} \sum_i^{\varepsilon_{t/2,K}} \varepsilon_i (\varepsilon_{i+1} - \varepsilon_i) [\sigma(\varepsilon_{i+1}) \cdot \sigma(\varepsilon_i)] = M(\kappa) \quad (3.2)$$

Eq. (3.2) shows the moment applied to the specimen when it is bent with a specific curvature. Also, through this Eq. (3.2), the stress-strain data obtained from the tensile test is converted into moment-curvature data, and the diagram shown is shown in Fig. 3.13.

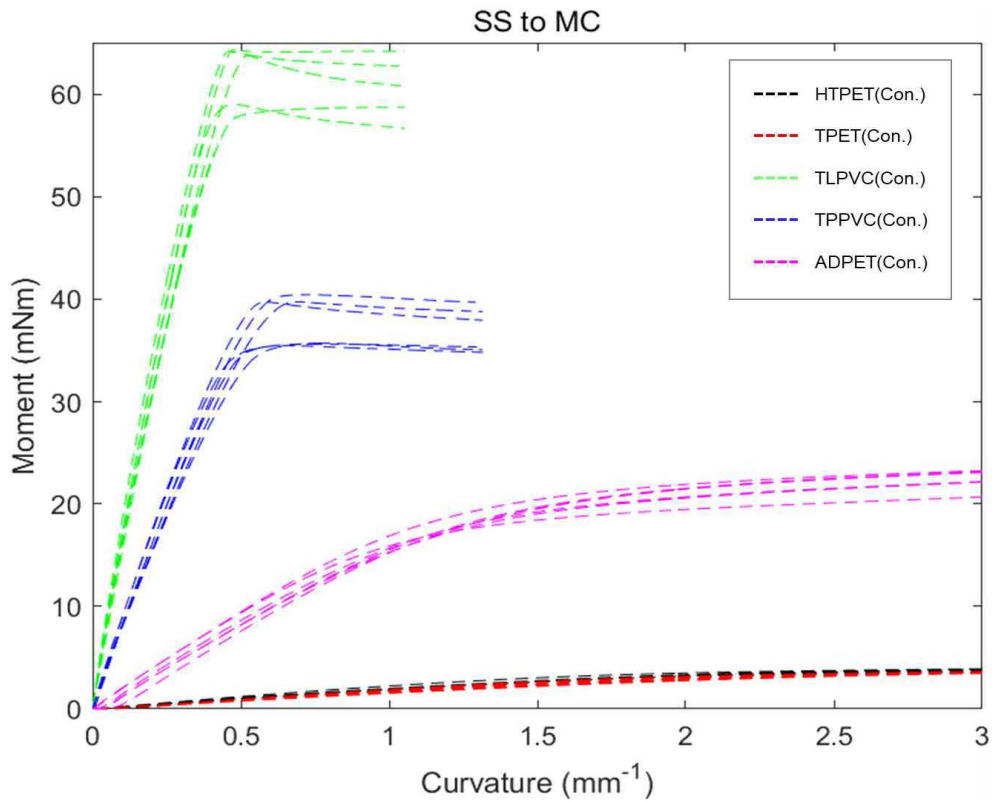


Fig. 3.13 Moment-curvature diagram (Converted from tensile test)

The results of converting stress strain data from the tensile test into moment-curvature data and the moment-curvature data from the bending test are shown in Fig. 3.14.

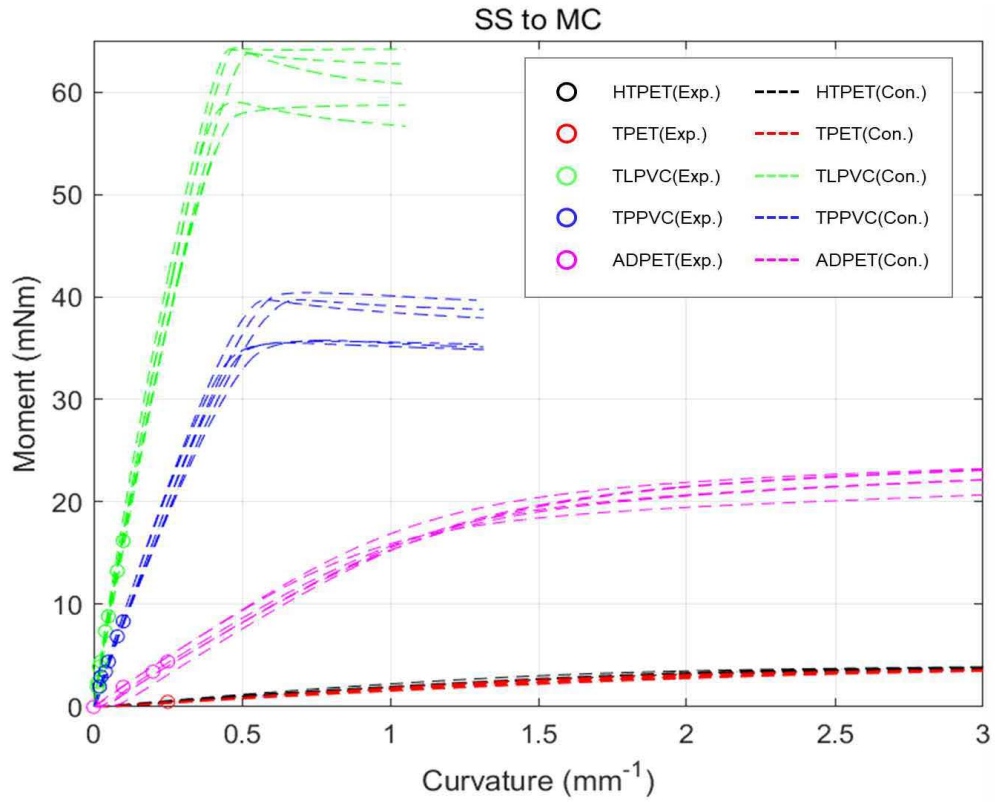


Fig. 3.14 Moment-curvature diagram (Tensile test conversion and bending test)

The moment-curvature data obtained from the bending test overlaps with the moment-curvature data obtained from the conversion from the tensile test are shown in Fig. 3.14. In addition, the results of enlarging the small curvature (<0.3) range in Fig. 3.14 are shown in Fig. 3.15.

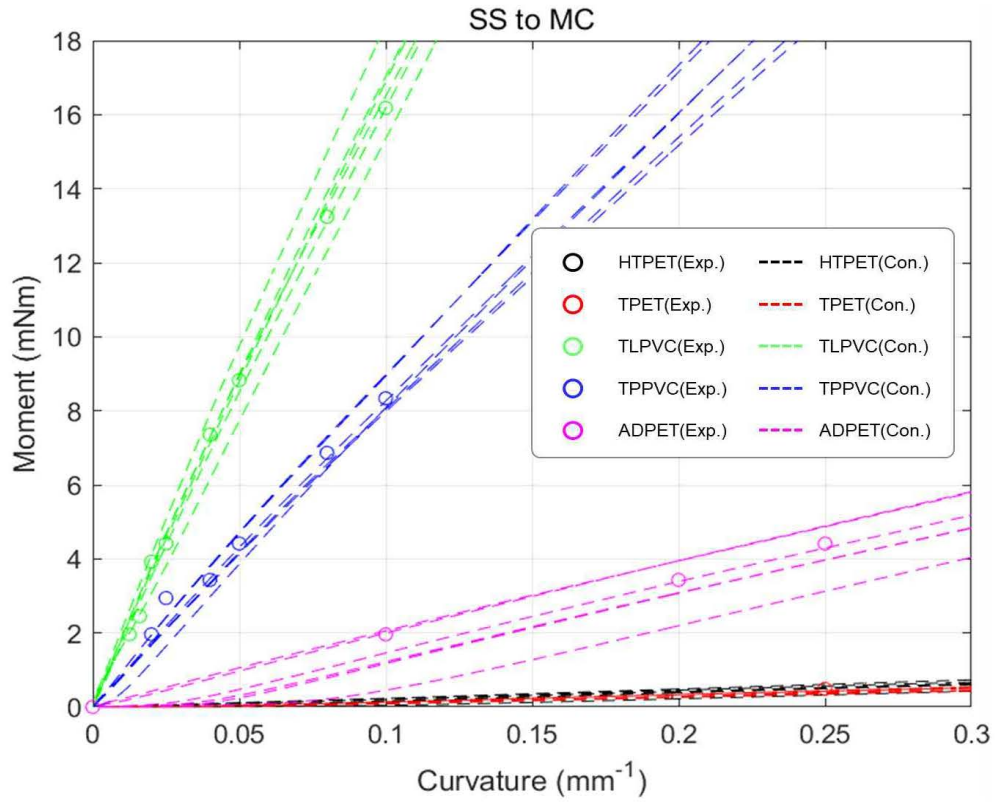


Fig. 3.15 Enlarge view of moment-curvature diagram (Tensile test conversion and bending test)

The results obtained from the pure bending test are within the range of six conversion data for each material obtained through three tensile tests in two directions are shown in Fig. 3.15. Therefore, it can be concluded that the pure bending test equipment has secured reliability by comparing the moment-curvature diagram, which is the second verification of the manufactured pure bending test equipment.

3.5 Material nonlinearity

The results of the experiment through the designed pure bending equipment are shown in Fig. 3.3, which can be said to measure only the material linearity. Therefore, additional experiments were performed to material whether material nonlinearity could be measured using the designed pure bending equipment.

In order to check whether the nonlinearity of the material can be measured using the designed pure bending equipment, a pure bending experiment was performed with four layers specimens of TLPVC and TPPVC using adhesives. The moment-curvature data obtained using the single layer and four layers specimens of TLPVC and TPPVC as materials for pure bending tests are shown in Fig. 3.16. The data marked with 'O' marks are the results of single layer specimens, and the data marked with 'X' marks are the results of four layers specimens.

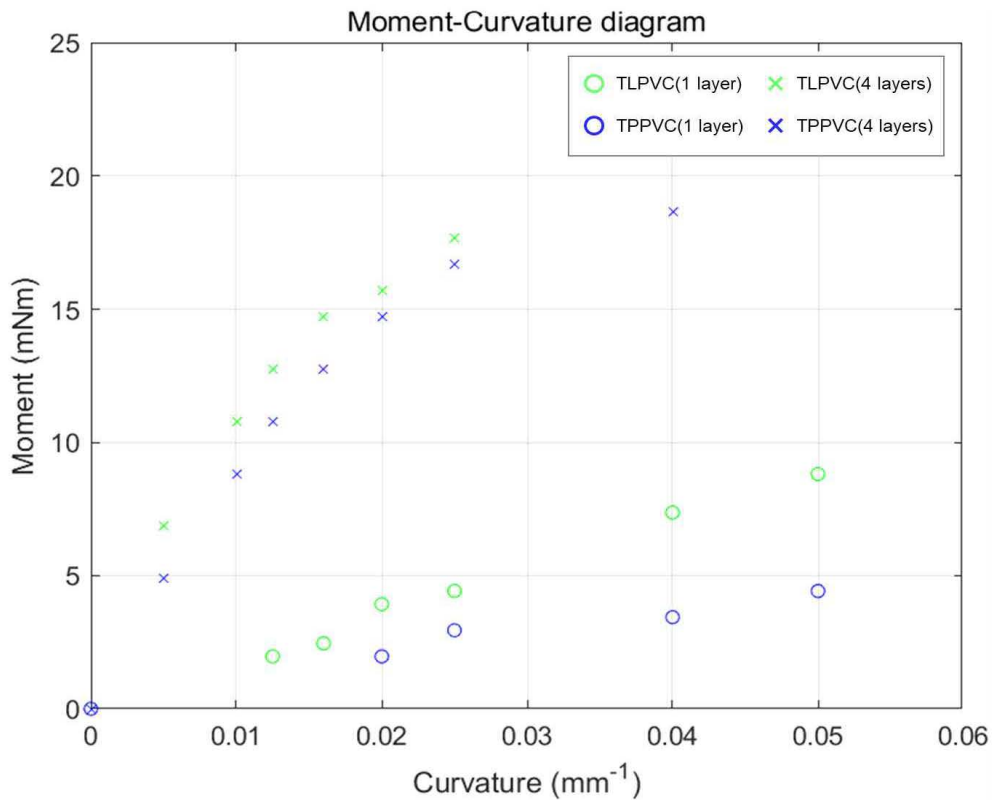


Fig. 3.16 Moment-curvature diagram (Single layer and four layers)

The bending test results of the four layers specimens (TLPVC and TPPVC) showed that the moment-curvature data were nonlinear. Unlike the single layer specimens, the result is nonlinear because the adhesive applied between each layer caused slip on the four layers specimens, and it can be expected that the material law was not constant due to this slip.

In addition, the results of regression of the measured moment-curvature data with a nonlinear model when using the four layers specimens are shown in Fig. 3.17. Non-linear models to which regression is applied are shown in Table 3.7. Based on the results shown in Fig. 3.16 and Fig. 3.17, it can be concluded that the material nonlinearity of the specimen can be measured using the experimental equipment designed.

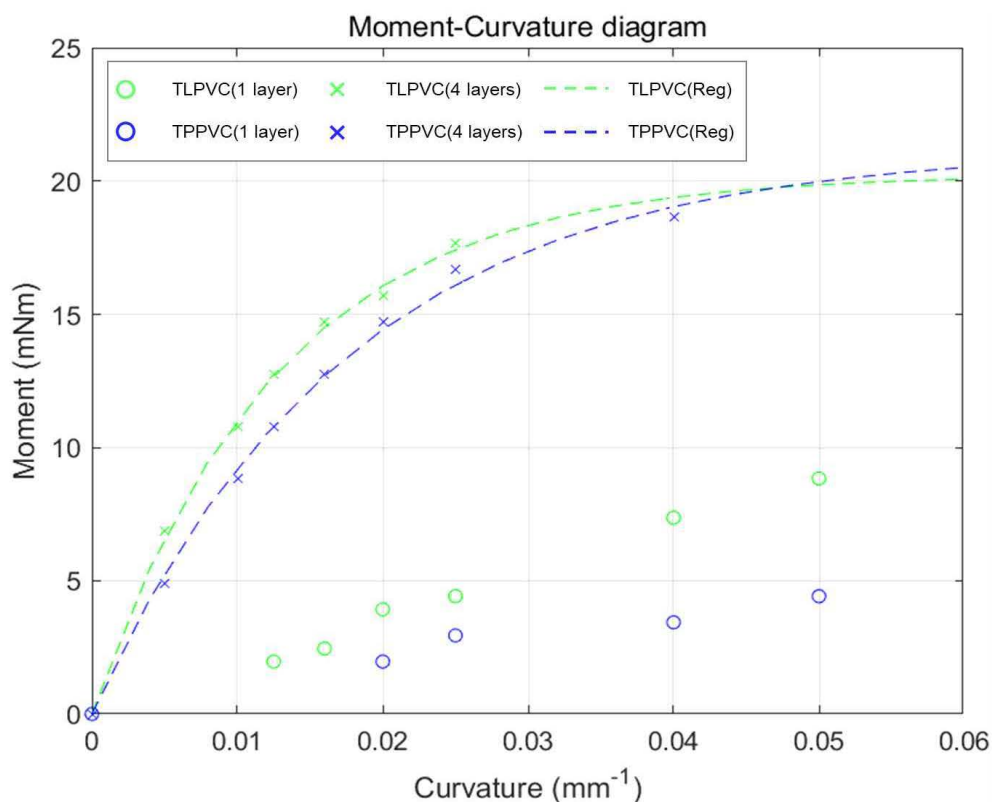


Fig. 3.17 Moment-curvature diagram with regression applied (Four layers)

Table 3.7 Regression results for each material (Four layers)

Material	Regression Model $f(x) = a(1 - e^{-bx})$
TLPVC	$f(x) = 20.25(1 - e^{-78.9x})$
TPPVC	$f(x) = 21.2(1 - e^{-57.11x})$

Chapter 4. Conclusions

Traditional pure bending equipment had problems that the specimens did not bend at a constant curvature along the specimen, did not apply a constant moment along the specimen, or could not perform the experiment in a large curvature range. To solve these problems, we developed a pure bending test equipment that can measure bending behavior for flexible and thin materials.

Using the designed equipment, we were able to derive a moment-curve diagram by measuring flexural rigidity and moment-curvature data, which are bending properties of five flexible and thin materials (HTPET, TPET, TLPVC, TPPVC, and ADPET).

Experimental verification was performed to ensure the reliability of the designed pure bending test equipment. For the first verification, the Young's modulus derived indirectly by performing a pure bending test and the Young's modulus derived directly by performing a tensile test were compared. For the second verification, the moment-curvature diagram derived directly from pure bending test and the moment-curvature diagram derived indirectly by converting stress-strain data obtained from tensile test were compared. The reliability of the designed pure bending test equipment was secured through two verifications.

In addition, four layers specimens (TLPVC, TPPVC) layered by applying an adhesive was used for the bending test to check whether the designed pure bending test equipment could measure the material nonlinearity. The moment-curvature data was nonlinear due to the slip of the adhesive applied between the layers, and since the moment-curvature data can be regressed by a nonlinear model, it was confirmed that the designed pure bending test equipment can measure the material nonlinearity.

According to the results shown in Table 3.3, it was necessary to measure more precisely in a small curvature range, and in a large curvature range, the measurement was discrete, so the moment could not be measured. More data can be obtained if the pure bending test equipment is designed to allow continuous measurement, and cyclic bending, relaxation and reverse loading tests are expected if the jig movement is automatically controlled, as illustrated in Fig. 4.1. In addition, in the process of designing pure bending test equipment, bending behavior can be measured for a larger curvature range if the thickness of the jig holding the specimen can be designed thinner.

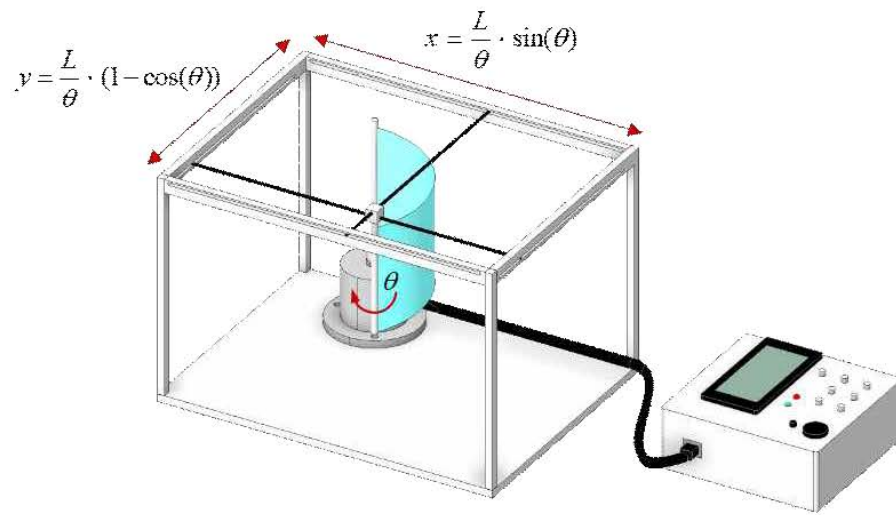


Fig. 4.1 Pure bending test equipment to be proposed in the future

Bibliography

- [1] S.H. Chae, W.J. Yu, J.J. Bae, D.L. Duong, D. Perello, H.Y. Jeong, Q.H. Ta, T.H. Ly, Q.A. Vu, M. Yun, Transferred wrinkled Al₂O₃ for highly stretchable and transparent graphene-carbon nanotube transistors, *Nature materials* 12(5) (2013) 403-409.
- [2] M. Kaltenbrunner, T. Sekitani, J. Reeder, T. Yokota, K. Kuribara, T. Tokuhara, M. Drack, R. Schwödiauer, I. Graz, S. Bauer-Gogonea, An ultra-lightweight design for imperceptible plastic electronics, *Nature* 499(7459) (2013) 458-463.
- [3] Y. Chen, J. Au, P. Kazlas, A. Ritenour, H. Gates, M. McCreary, Flexible active-matrix electronic ink display, *Nature* 423(6936) (2003) 136-136.
- [4] B. Lahey, A. Girouard, W. Burleson, R. Vertegaal, PaperPhone: understanding the use of bend gestures in mobile devices with flexible electronic paper displays, *Proceedings of the SIGCHI Conference on Human Factors in Computing Systems*, (2011), pp. 1303-1312.
- [5] J.E. Carlé, M. Helgesen, M.V. Madsen, E. Bundgaard, F.C. Krebs, Upscaling from single cells to modules-fabrication of vacuum-and ITO-free polymer solar cells on flexible substrates with long lifetime, *Journal of Materials Chemistry C* 2(7) (2014) 1290-1297.
- [6] M. Kaltenbrunner, M.S. White, E.D. Głowacki, T. Sekitani, T. Someya, N.S. Sariciftci, S. Bauer, Ultrathin and lightweight organic solar cells with high flexibility, *Nature communications* 3(1) (2012) 1-7.
- [7] A.M. Gaikwad, A.M. Zamarayeva, J. Rousseau, H. Chu, I. Derin, D.A. Steingart, Highly stretchable alkaline batteries based on an embedded conductive fabric, *Advanced Materials* 24(37) (2012) 5071-5076.
- [8] G. Zhou, F. Li, H.-M. Cheng, Progress in flexible lithium batteries and future prospects, *Energy & Environmental Science* 7(4) (2014) 1307-1338.
- [9] M.S. White, M. Kaltenbrunner, E.D. Głowacki, K. Gutnichenko, G. Kettlgruber, I. Graz, S. Aazou, C. Ulbricht, D.A. Egbe, M.C. Miron, Ultrathin, highly flexible and stretchable PLEDs, *Nature Photonics*

7(10) (2013) 811-816.

[10] C.L.C. Chien, Y.C. Huang, S.F. Hu, C.M. Chang, M.C. Yip, W. Fang, Polymer dispensing and embossing technology for the lens type LED packaging, *Journal of Micromechanics and Microengineering* 23(6) (2013) 065019.

[11] O. Kraft, C.A. Volkert, Mechanical Testing of Thin Films and Small Structures, *Advanced Engineering Materials* 3(3) (2001) 99-110.

[12] P. Curtis, CRAG test methods for the measurement of the engineering properties of fibre reinforced plastics, (1988).

[13] M. Wisnom, J. Atkinson, Reduction in tensile and flexural strength of unidirectional glass fibre-epoxy with increasing specimen size, *Composite Structures* 38(1-4) (1997) 405-411.

[14] Ş. Karakaya, Ö. Soykasap, Homogenized tensile and bending properties of plain weave single-Ply E-glass/epoxy, *Polymer composites* 33(6) (2012) 881-888.

[15] A. Perduijn, S. Hoogenboom, The pure bending of sheet, *Journal of Materials Processing Technology* 51(1-4) (1995) 274-295.

[16] M. Elchalakani, X.L. Zhao, R.H. Grzebieta, Concrete-filled circular steel tubes subjected to pure bending, *Journal of constructional steel research* 57(11) (2001) 1141-1168.

[17] J. Muñoz-Guijosa, V. Rodríguez de la Cruz, D. Fernández Caballero, A. Díaz Lantada, J. Echávarri Otero, Simple testing system for pure bending tests with large deflections, *Experimental mechanics* 52(7) (2012) 679-692.

[18] F. Yoshida, M. Urabe, V. Toropov, Identification of material parameters in constitutive model for sheet metals from cyclic bending tests, *International journal of mechanical sciences* 40(2-3) (1998) 237-249.

[19] G. Arnold, S. Calloch, D. Dureisseix, R. Billardon, A pure bending machine to identify the mechanical behaviour of thin sheets, 6th. International ESAFORM Conference on Material Forming,

2003, pp. 1-4.

[20] S. Boers, M. Geers, V. Kouznetsova, Contactless and frictionless pure bending, *Experimental Mechanics* 50(6) (2010) 683-693.

[21] J. Duncan, S.C. Ding, W.L. Jiang, Moment-curvature measurement in thin sheet-part I: equipment, *International Journal of Mechanical Sciences* 41(3) (1999) 249-260.

[22] M. Weiss, H. Wolfkamp, B. Rolfe, P. Hodgson, E. Hemmerich, Measurement of bending properties in strip for roll forming, international deep drawing research group (2009) 521-532.

[23] M. Weiss, B. Abeyrathna, D.S. Gangoda, J. Mendiguren, H. Wolfkamp, Bending behaviour and oil canning in roll forming a steel channel, *The International Journal of Advanced Manufacturing Technology* 91(5) (2017) 2875-2884.

[24] G. Sanford, A. Biskner, T. Murphey, Large strain behavior of thin unidirectional composite flexures, 51st AIAA/ASME/ASCE/AHS/ASC Structures, Structural Dynamics, and Materials Conference 18th AIAA/ASME/AHS Adaptive Structures Conference 12th, (2010), p. 2698.

[25] J. Mendiguren, A. Abvabi, B. Rolfe, M. Weiss, Improvement of accuracy in a free bending test for material characterization, *International Journal of Mechanical Sciences* 103 (2015) 288-296.

[26] ASTM D790, Standard test methods for flexural properties of unreinforced and reinforced plastics and electrical insulating materials, Annual book of ASTM Standards, 1997.

[27] ASTM 6272, Standard Test Method for Flexural Properties of Unreinforced and Reinforced Plastics and Electrical Insulating Materials by Four-Point Bending, Annual book of ASTM Standards, 2010.

[28] ASTM 7264, Standard Test Method for Flexural Properties of Polymer Matrix Composite Materials, Annual book of ASTM Standards, 2015.

[29] T. Weihs, S. Hong, J. Bravman, W. Nix, Mechanical deflection of cantilever microbeams: A new technique for testing the mechanical properties of thin films, *Journal of Materials Research* 3(5) (1988)

931-942.

[30] J.Ä. Schweitz, Mechanical characterization of thin films by micromechanical techniques, MRS bulletin 17(7) (1992) 34-45.

[31] J. Lewis, S. Grego, E. Vick, B. Chalamala, D. Temple, Mechanical performance of thin films in flexible displays, MRS Online Proceedings Library 814(1) (2004) 307-316.

[32] L. Landau, E. Lifshitz, Theory of Elasticity, Vol. 7. 3rd, Elsevier, 1986.

[33] J. Hu, Z. Marciniak, J. Duncan, Mechanics of sheet metal forming, Elsevier, 2002.